American Society of Mechanical Engineers

ASME Accepted Manuscript Repository

Institutional Repository Cover Sheet

Serena Graziosi
First *Last*

ASME Paper Title: The design process of additively manufactured mesoscale lattice structures: A review

Authors: Francesco Tamburrino, Serena Graziosi, Monica Bordegoni

ASME Journal Title: Journal of Computer and Information Science in Engineering

Volume/Issue: 18(4) Date of Publication (VOR* Online): July 3, 2018

ASME Digital Collection URL: https://asmedigitalcollection.asme.org/computingengineering/article/18/4/040801/36
Design-Process-of-Additively-Manufactured

DOI: 10.1115/1.4040131

This content is ASME © provided under the ASME ©; CC-BY distribution license

*VOR (version of record)

The design process of additively manufactured Meso-Scale Lattice Structures: a review

Francesco Tamburrino
Department of Mechanical Engineering
Politecnico di Milano
Milan, 20156
Italy
Email: francesco.tamburrino@polimi.it

Serena Graziosi *
Department of Mechanical Engineering
Politecnico di Milano
Milan, 20156
Italy
Email: serena.graziosi@polimi.it

Monica Bordegoni
Member of ASME
Department of Mechanical Engineering
Politecnico di Milano
Milan, 20156
Italy
Email: monica.bordegoni@polimi.it

ABSTRACT

This review focuses on the design process of additively manufactured Meso-Scale Lattice Structures (MSLSs). They are arrays of 3D printed trussed unit cells, whose dimensions span from 0.1 to 10.0 mm. This study intends to detail the phases of the MSLSs design process (with a particular focus on MSLSs whose unit cells are made up of a network of struts and nodes), proposing an integrated and holistic view of it, which is currently lacking in the literature. It aims at guiding designers' decisions with respect to the settled functional requirements and the manufacturing constraints. It also aims to provide an overview for software developers and researchers concerning the design approaches and strategies currently available. A further objective of this review is to stimulate researchers in exploring new MSLSs functionalities, consciously considering the impact of each design phase on the whole process, and on the manufactured product.

Nomenclature

b Number of struts of the unit cell, Section 3.1
D Strut diameter, Section 3.1
D_{max} Strut maximum diameter, Section 3.2
D_{min} Strut minimum diameter, Section 3.2
D_f Strut diameter variation, Section 3.2
E Young's modulus
G Shear modulus
H Unit cell height, Section 3.1
I Area moment of inertia, Section 3.1
j Number of joints/nodes of the unit cell, Section 3.1
L Strut length, Section 3.1
L_{max} Strut maximum length, Section 3.2
L_{min} Strut minimum length, Section 3.2
M Maxwell's criterion, Section 3.1
m Number of independent inextensional mechanisms, Section 3.1

*Address all correspondence related to ASME style format and figures to this author.

MSLS Meso-Scale Lattice Structure, Section 1
R_h Horizontal deflection ratio, Section 3.2
R_s Sloped deflection ratio, Section 3.2
s Number of independent self-stress states, Section 3.1
t Strut thickness, Section 3.1
t_{max} Strut maximum thickness, Section 3.2
t_{min} Strut minimum thickness, Section 3.2
t_a Strut thickness along the *a* direction, Section 3.2
t_b Strut thickness along the *b* direction, Section 3.2
W Unit cell width, Section 3.1
θ Strut sloping angle, Section 3.2

1 Introduction

The word *lattice* has been already used in various contexts and with different meanings (see Figure 1). In crystallography (i.e., in the *micro-scale*), a lattice is graphically represented as a grid of connected lines; the intersections among these lines identify the sites of the atoms within the crystal [1]. In civil engineering and architecture (i.e., in the *macro-scale*) a *lattice structure* represents an array of struts, pin-jointed or stiffly bonded at their connections [2]. In this paper, we will use the word *lattice* in a different dimensional scale, i.e., the *meso-scale* (see Figure 1). We will use the expression Meso-Scale Lattice Structures (MSLSs) to identify those structures of *cellular materials* having the following characteristics: the unit cell dimensions span from 0.1 to 10.0 mm [3]; the unit cell structure is made up of a *network of trussed struts* or, a *triply periodic minimal surface* or, a *wall-based structure* or, it has a *custom geometry* (see Figure 2); the structures are built using Additive Manufacturing (AM) technologies.

The structures of *cellular materials*, can be divided into two main categories (see [4]) on the basis of the way their unit cell is spatially arranged: *stochastic* and *non-stochastic* (see Figure 2). Cellular materials, characterized by a stochastic distribution of their unit cells, are the open and closed foams. Such uncontrolled distribution is mainly a consequence of the manufacturing process of this material. It is based on the injection of gases like air, nitrogen, and argon or on the addition of blowing agents that decompose and release gas when the material foam is molten [5]. These gases or blowing agents generate very fine bubbles inside the foam. Using sophisticated mixing techniques, based on rotating motors, the distribution of these bubbles can be roughly, but not totally, controlled [6]. Open foams have energy-absorbing capabilities while, closed foams, are usually characterized by stiffness and strength [6].

Cellular materials having non-stochastic structures are characterized by a controlled organization of their unit cells. The unit cell arrangement can be both 2D or 3D (see Figure 2). As 2D non-stochastic structures we have mainly wall-based MSLSs. According to Maxwell's stability criterion (it will be discussed in Section 3.1, see also [1]), they can be stiff or soft. As 3D non-stochastic structures we can mention (see also Figure 2 and [4]): Voronoi; TPMS (Triply Periodic Minimal Surface); 3D strut-and-node based lattices; 3D custom structures.

Voronoi patterns could appear as stochastic structures since they are built through nonuniform geometric modules. Instead, their arrangement is controlled by mathematical and geometric principles. Indeed, a Voronoi pattern is based on the partition of a plane, starting from a preset number of generating points, into polygons; to each point corresponds a polygon which is built around it. The points belonging to the polygon contour are the ones closest to the generating point [7].

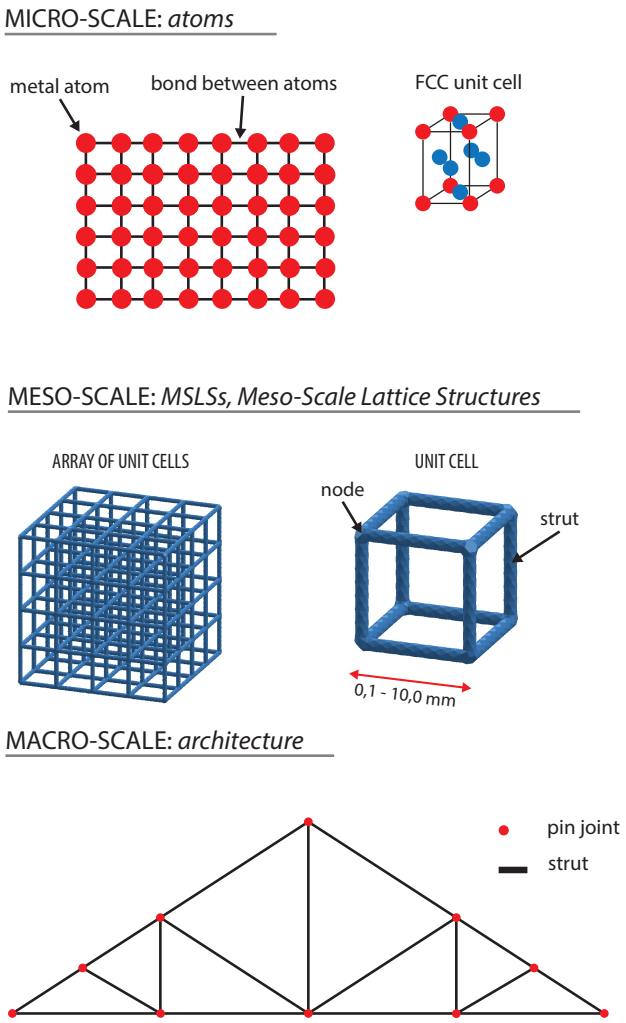

Fig. 1: The concept of *lattice* applied to different dimensional scales: structures defining the atoms arrangement in the micro-scale; structures of cellular materials in the meso-scale; specific architectural structures in the macro-scale.

They are mostly used for structural applications in architecture and civil engineering, and they are often characterized by a stiff mechanical behavior [8, 9]. *TPMS structures* are based on fixed and mainly organic geometries, often inspired by the observation of living organisms and nature [10, 11]. They can be mainly used for generating lightweight structures characterized by a high surface area which provides to these structures heat exchange and noise control capabilities [11, 12]. One of the advantages of *TPMS structures* is that they do not suffer local stress concentrations which is instead more frequent in strut-and-node based ones [13]. *3D strut-and-node based lattice structures* are characterized by a strut-and-node arrangement and, again, they can be stiff or soft. Finally, *3D custom structures* are those whose unit cells are designed usually starting from simple solid geometries (e.g., a sphere or a cube) upon which boolean operations are applied to shape the internal void (an example is provided in Figure 2). The mechanical behavior of these structures can thus vary since it depends on the geometry of the unit cell.

This review will be focused on discussing the design process of *3D strut-and-node based MSLSs* (Figure 2). Despite AM technologies give the possibility to work on mesoscale, having high control over the object dimensions and using and combining a wide range of materials (polymers, metals, ceramics, etc.) [15] however, the most widespread additively manu-

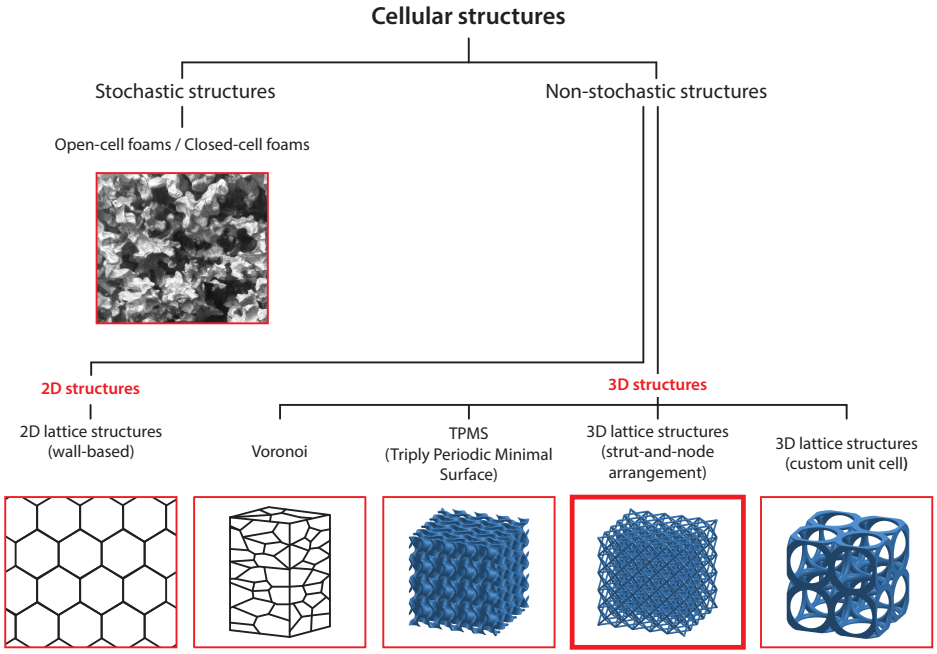

Fig. 2: Cellular structures can be divided into stochastic and non-stochastic ones. Both the arrangement as well as the geometry of the unit cells of 2D and 3D non-stochastic structures can be designed. This paper is focused on the design process of *3D strut-and-node based lattice structures*. This type of cellular structure is highlighted in the image. This figure is inspired by [4], page 325, while the TPMS structure has been modeled using the software, developed at the University of Nottingham, mentioned in [14].

factured MSLSs are the ones made of mono-material linear struts. Nevertheless, even if the examples and the considerations provided will be focused on this kind of non-stochastic structures, the main phases of the design process can be considered valid also for the others (see Figure 2) with the exception of the Voronoi pattern whose generation undergoes specific rules (e.g., see [16]).

The aim of this review is to reflect upon the MSLSs design workflow clarifying and detailing the various phases. Indeed, the available literature on the design of MSLSs is mainly focused on discussing a specific phase of the process: an integrated and holistic view is currently lacking. To create such a view, this work has been conceived to build a link among the main research findings available in the literature and related to the design and manufacturing of MSLSs. This link is a proposal of a design workflow through which the consequences of each design choice, on the whole process, are made explicit.

Starting from the desired functionalities of the structure to be printed and the design space to be filled, this review has the goal to show and explain how the decisional process is structured, what are the parameters to be managed and how each design choice influences the final result. Critical observations and possible future perspectives are proposed to have broad control over the MSLSs design process, avoiding the relocation of design issues from a phase to another. A further contribution of this review is also to provide a homogenization and disambiguation of the terminology used in this field since for example, words such as *lattice* have different meanings according to the context they are being used (e.g., see Figure 1).

We believe that this review can be beneficial for various experts working in the AM field. Designers could retrieve indications for better structuring their decisional process when looking for the most suitable MSLS configuration with respect to functional and manufacturing constraints. Software developers could get insights for the development or tuning of design

tools. Researchers could get a comprehensive view on the topic together with indications for developing more integrated and evolutionary design approaches.

After this initial introduction, the paper presents, in Section 2, the phases of the MSLSs design process. These phases will be used as the thread of our discussion and thus, to structure the Section 3 where the main contributions available in the literature are reviewed. In Section 4 the discussion is focused on the analysis of the innovative functionalities that these structures can provide. Finally, in Section 5 conclusions are drawn.

2 The phases of the MSLSs design workflow

The MSLSs design workflow is represented in Figure 3. Once identified the design space to be used, the process begins with the specifications of the functional capabilities that the MSLS will have to provide to the component/object. Indeed, following the principles of Design For Additive Manufacturing (DFAM) as defined by Chu et al. [17], the intent is to exploit the potentialities of these technologies fostering a local and punctual control of the material distribution. This fact implies not only the possibility to have a more efficient material distribution (i.e., only where needed) but also to provide further functionalities to the object. Concerning these functionalities, in this work, we will mostly refer to the mechanical behavior (stiff, ductile, etc.) of the object even if in Section 4 further examples will be provided.

Once settled the functional targets, the first design phase consists in the *"Unit cell design or selection"*. We can distinguish two main classes of unit cells: *stretch-dominated* which are stiff and suitable for lightweight structural applications; *bending-dominated* which are soft and suitable for energy-absorbing applications [18]. This choice can be made by analyzing the strut-and-node arrangement, i.e., applying Maxwell's stability criterion (see Section 3.1 and [1]). Another aspect to be considered, when designing the unit cell, is the loading direction with respect to the strut-and-node arrangement, i.e., the mechanical behavior required along each direction [3]. As it will be discussed in Section 3.1, the unit cell geometry can be optimized taking also into account this aspect. The output of this phase is the 3D sketch representation of the unit cell.

The second phase of the workflow refers to the *"Preliminary unit cell sizing"*. During this phase, a preliminary choice of the dimensions of the unit cell is performed implementing the manufacturing constraints in terms of minimum and maximum length of the struts, self-supporting sloping angles and minimum diameters or thicknesses [19]. Together with these geometric constraints, necessary to guarantee the technical feasibility of the printing process, there are also other manufacturing aspects (they will be discussed in Section 3.2) to be considered for guaranteeing the final quality of the structure [20]. The output of this phase is the 3D model of the unit cell, whose struts have all the same thickness/diameter.

Once the unit cell dimensions are known the next phase consists in the *"Population of the design space"*. During this step, an array of unit cells is generated to fill a volume (i.e., the design space). There are two main strategies to pursue (see Section 3.3): performing a uniform or a conformal distribution [3] of these unit cells within the design space. In the first case, the unit cells distribution is matrix based; it does not take into account the boundary of the design space. Hence, boolean operations are needed to remove those parts of the structure which exceed the design space. In the second case, the filling operation automatically adapts the geometry of the cells to take into account the geometric boundary of the design space. The output of this phase is the 3D model of a homogeneous MSLS (each strut has the same thickness/diameter).

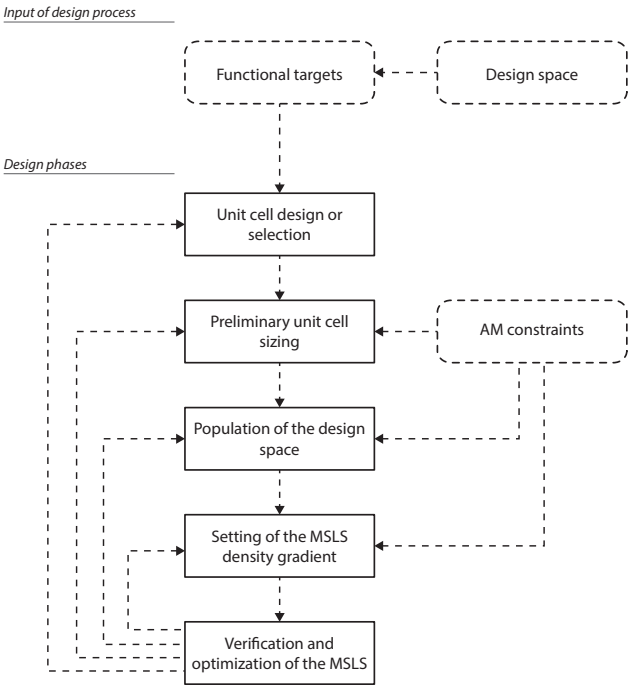

Fig. 3: The Meso-Scale Lattice Structures (MSLSs) design workflow. Starting from the available design space and the functional targets to be reached, the design process is then structured into five main phases. During these phases manufacturing constraints will also be taken into account to guarantee the printability of the structure.

The following phase consists in finalizing the geometric characteristics of the MSLS. The last design aspect to be decided is the *"Setting of the MSLS density gradient"*, which at this point of the design phase (i.e., when the unit cell has been already selected), depends only on the thickness/diameter of the struts. There are three main possible situations. If the current relative density of the MSLS is appropriate, we can move to the next design phase. On the contrary, if the relative density of the structure needs to be modified, we can vary the material distribution by modifying the diameter/thickness of the struts. This variation can be homogeneous or heterogeneous. In this first case, the diameter/thickness of all the struts undergoes the same change (i.e., they are scaled). In the second case, we can locally vary this value applying a heterogeneous gradient of density [21]. As it will be discussed in Section 3.4, the application of the gradient enables the modification of the thickness/diameter of the struts taking into account the distribution and the intensity of the mechanical stress acting on the MSLS [22–24]. To perform this activity, it can be, again, necessary to take into account the manufacturing constraints. For example, in case of powder-based printing technologies, it is important to guarantee an easy removal of the not melted or not sintered powder: an excessive increase of the struts thickness or diameter could make this removal quite complex since the dimensions of the empty volumes will decrease. The output of this phase is the 3D model of a MSLS characterized by a specific relative density.

The final step of the process consists in the *"Verification and optimization of the MSLS"*. This phase has the purpose of validating the behavior of the structure. As it will be shown in Section 3.5, simulations can also be adopted during the previous phases of the design process, with the intent of developing and optimizing the material distribution and thus, the design of the cell, and of the resulting MSLS [25].

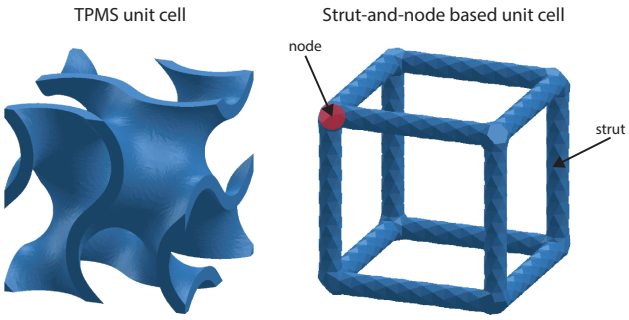

Fig. 4: Two examples of unit cells: a TPMS (cell modeled using the software, developed at the University of Nottingham, mentioned in [14]) and a 3D strut-and-node based cell.

3 Review of the MSLSs design phases

In this Section, all the phases represented in Figure 3 are reviewed and analyzed taking into account the most relevant literature in this field. The Section ends with a part dedicated to the modeling issues.

3.1 Unit cell design or selection

As anticipated in Sections 1 and 2, the unit cell is the primary module of a MSLS. Hence, the design or the selection of the unit cell represents the first phase of the design process (see Figure 3).

The categories of unit cells that can be considered as the primary and most known are: the TPMS and the strut-and-node based one, as defined in [26]. They are represented in Figure 4. The TPMS cell can be further split into two subcategories or phases, called matrix and network [26]. Matrix unit cells are made up of a solid wall, bounded by two unconnected empty regions. Network unit cells, instead, consist of only one solid and one hollow region. TPMS cells are based on fixed geometries like gyroid, Schwarz primitives, lidinoid, etc., characterized by continuous and often organic shapes [27]. They are, in fact, of particular relevance in natural sciences, having been observed for biological membranes, blocks of copolymers, etc. [10, 11]. For any TPMS geometry, both a matrix phase and a network phase can exist [26–28].

As anticipated in Section 1, strut-and-node based MSLSs are the focus of this review. This choice has been made because of the broad range of designing and developing possibilities that this kind of unit cell can offer, starting from its primary element (i.e., the strut), whose size, position, density, and inclination can be varied. On the contrary, the geometry of the TPMS cells is fixed (but it can be obviously scaled), and what can be altered is their density.

Ashby [1] defined strut-and-node based unit cells as a network of trussed struts pin-jointed or stiffly bonded at their connections. These unit cells can be divided into two categories: *stretch-dominated* and *bending-dominated* [1]. *Stretch-dominated* unit cells are characterized by high stiffness; conversely, *bending-dominated* cells have high strainability that makes them suitable for energy-absorbing applications [29]. The most commonly used lattice structures have a stiff mechanical behavior, and they are used for a wide range of structural applications where also lightweight is required [30]. A fundamental constructive aspect that determines opposite mechanical properties for stretch and bending-dominated unit cells is the level of connectivity of the joints, which is meant as the number of struts connected at joints [1]. *Stretch-dominated* unit cells are characterized by high connectivity, conversely the *bending-dominated* by low connectivity. *Stretch-dominated*

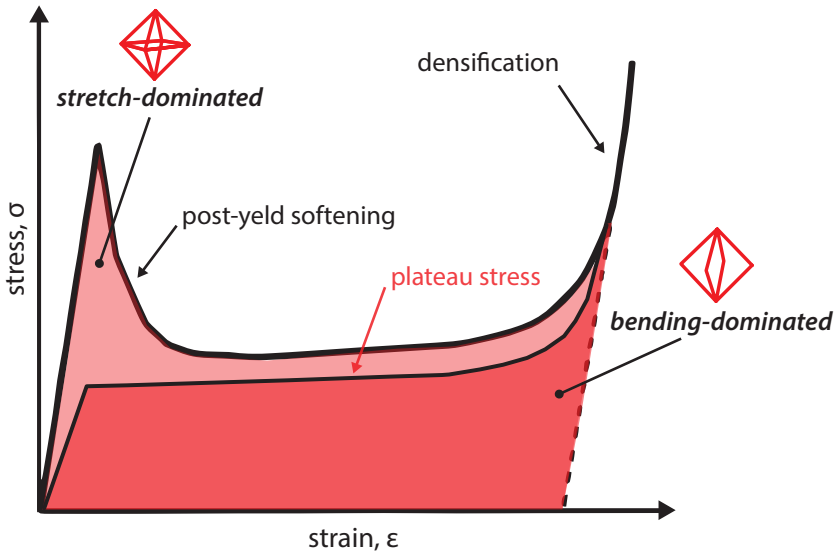

Fig. 5: The qualitative stress/strain curves of *stretch-dominated* and *bending-dominated* unit cells. The stress/strain curve of *stretch-dominated* unit cells is characterized by high stiffness and high initial strength, followed by post-yield softening. The stress/strain curve of *bending-dominated* unit cells is characterized by a lower stiffness, a lower initial strength and a large deformation at relatively low and constant stress (plateau stress). The last part of both curves shows the densification phase, that is the moment when the struts merge. The image is inspired by the work [1], pages 19 and 26.

and *bending-dominated* unit cells present different and characteristic stress/strain curves [1]. They are shown in Figure 5. For the first, after an elastic strain, a yielding occurs (plastic or brittle according to the nature of the material used), and then there is a post-yielding softening. In *bending-dominated* lattice structures, instead, after the yielding, there is (at relatively low levels of stress) a flat and extended stress plateau that is the main responsible for their characteristic energy-absorbing behavior. The last step of the stress/strain curve of a lattice structure is the densification phase, that is the moment when, under the load, the struts merge [4].

The high or low struts connectivity is not a quantitative and sufficient element to define and characterize the mechanical behavior of a unit cell (i.e., whether this one is bending or stretching). To this aim, and as already introduced by Ashby in [1], the Maxwell's criterion (M) can be used for both two-dimensional (see Equation (1)) as well as three-dimensional cells (see Equation (2)), as shown in Figure 6.

$$M = b - 2j + 3 = 0 \tag{1}$$

$$M = b - 3j + 6 = 0 \tag{2}$$

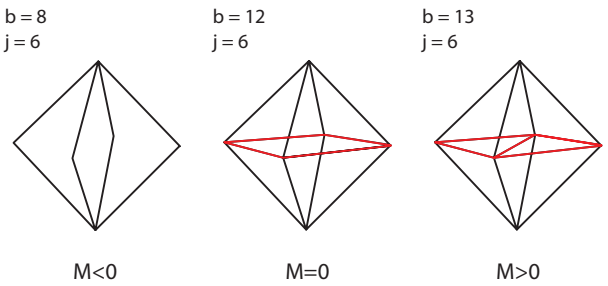

Fig. 6: Maxwell's Criterion (see Equation 2). The unit cell on the left has $M<0$: it is *bending-dominated* (nodes are all locked). The unit cell in the centre has $M=0$: it is *stretch-dominated*. Adding a further strut to this cell will make $M>0$. In this case, if nodes are unlocked there is a state of self-stress: the struts carry stress also if no external loads are applied. If nodes are locked, the cell is still *stretch-dominated* and can be manufactured using AM technologies. Figure inspired by [1] page 24.

where b is the number of struts creating the cell, and j the number of joints/nodes connecting these struts.

Three kinds of unit cells, having different mechanical behaviors according to Maxwell's criterion, are shown in Figure 6. When $M<0$, if nodes are locked joints (e.g., as the ones in Figure 4), and the unit cell is loaded, it strains (the cell is *bending-dominated*, see [1]). If joints are unlocked (e.g., nodes are hinges), and the unit cell is loaded, the cell folds (the cell behaves like a *mechanism)*. When $M=0$, the unit cell is *stretch-dominated* both if joints are locked or unlocked (see also [1]). When $M>0$, the cell is *over constrained* (see [1]) and states of self-stress occur [1]. They occur when the cell is built having, for example, struts shorter than the others which pulls these into compression without the need of any further external load: the struts carry the stress even though the unit cell is not under external loads (see [31]). For this kind of structures the following generalization of Maxwell's criterion has to be used (see [1, 31]):

$$M = b - 3j + 6 = s - m \tag{3}$$

where s is the number of *independent states of self-stress* and m the number of *independent inextensional mechanisms* (as defined in [31], see also [1, 32]). For a detailed explanation of how s and m values can be calculated see [31]. Hence, the Equation 3 is not applicable to unit cells of MSLSs as defined in this paper since we are considering the nodes of the cell as locked. However, the $M>0$ condition is still valid and still represents *stretch-dominated* structures since we are able to print cells like the one represented in Figure 6 (right) without generating *independent states of self-stress.* Finally, it is worth underlying that the Maxwell's criterion can be applied to unit cells having linear struts.

Among cellular structures, open foams belong to the category of *bending-dominated* ones and, thus, they can easily strain and absorb high quantities of energy. As anticipated in Section 1, their behavior is mainly due to their stochastic nature

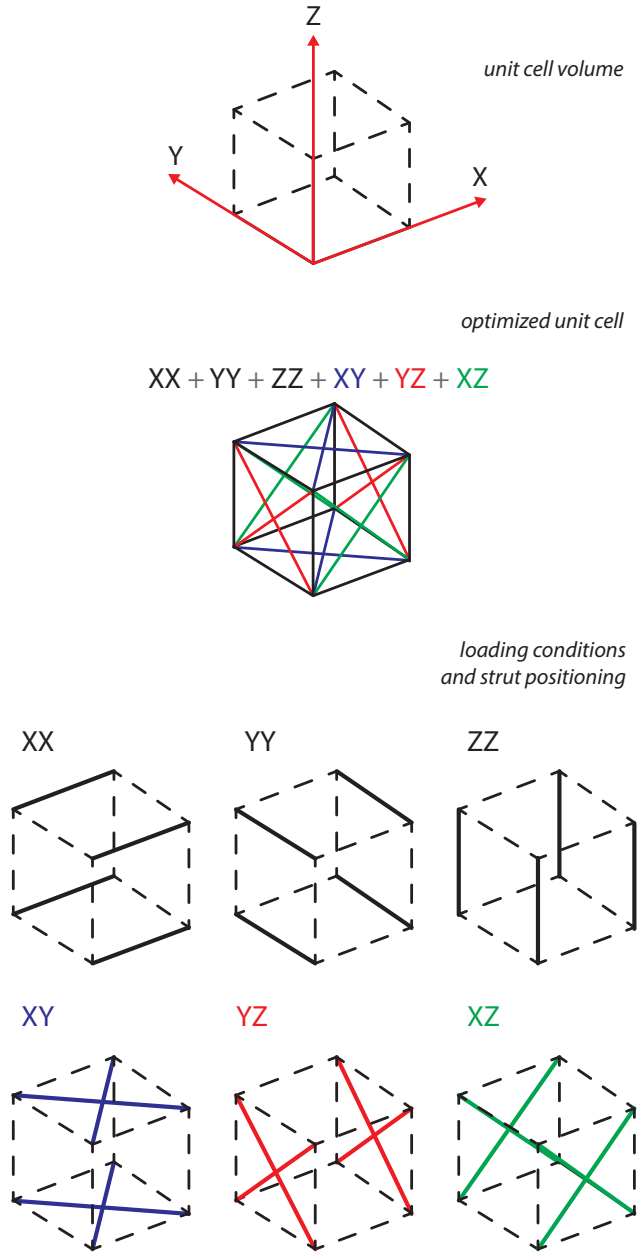

Fig. 7: Unit cell optimization according to six loading conditions (xx, yy, zz, yz, xy, xz). Considering, as design requirements, the stiffness and the strength as well as the loading conditions, the unit cell is optimized through a proper strut positioning for each loading condition. The combined results lead to the final cell developed and optimized in all directions. Figure inspired by [3] page 153.

and to their manufacturing process that creates heterogeneous structures, where both stiff and soft ”parts” can be found. The random arrangement of the struts, and of the stiff and soft *parts*, are responsible for the global bending behavior which is typical of foams [33]. On the contrary, strut-and-node based cells can be both *bending-dominated* or *stretch-dominated*. This feature gives us the possibility to properly design the mechanical behavior of these cells considering the functional targets set at the beginning of the design process.

Once the identification of the desired unit cell has been performed (i.e., *bending-dominated* or *stretch-dominated*), then, the geometry of the unit cell, as suggested by Nguyen et al. [3] and, as shown in Figure 7, can be further tuned. This tuning

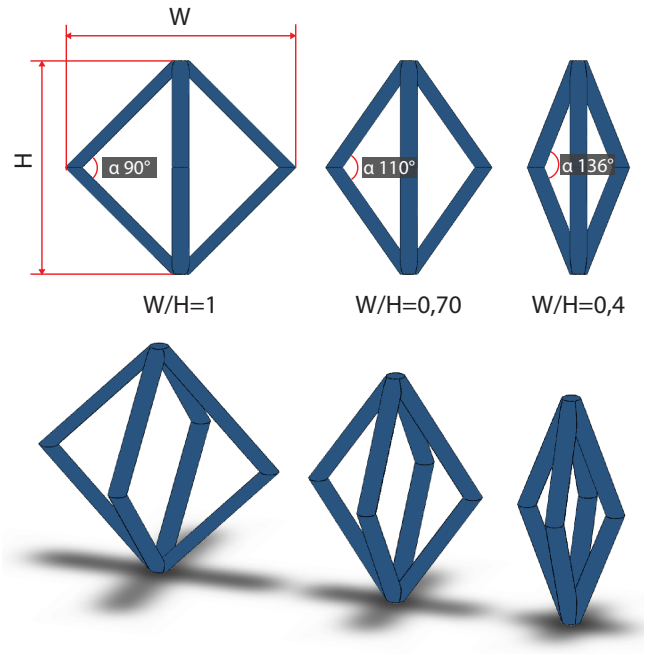

Fig. 8: The aspect ratio of a BCC unit cell. When W and, thus, the aspect ratio (W/H) decreases, the unit cell shows higher stiffness and yield stress. In particular, the amplitude of the angles between the struts changes. The amplitude of the angles at the bottom, and at the top of the unit cell, decreases while, for the angles at the sides (α) of the unit cell, the amplitude increases. This figure is used to summarise some considerations provided in [34].

can be done considering the loading conditions of the cell and thus, optimizing the position/orientation of the struts. To perform this activity an approach that analyzes and improves the strut-and-node arrangement, according to the directions of loads, can be used [3]. Indeed Nguyen et al., in [3], describe the following approach. They apply six loading conditions (xx, yy, zz, yz, xy, xz) and set some *optimization parameters* (i.e., strain energy constraints, Poisson's ratio, elastic modulus, loading magnitude) in ANSYS (www.ansys.com). For each loading direction, the unit cell is optimized. The combination of these results leads to a unit cell whose structure is tuned with respect to the loading directions (see also Figure 7). For each kind of unit cell of the study and all loading directions, the results associated with the strain energy are calculated and normalized with a value between 0 and 1 [3].

A further example of unit cell development is described by Smith et al. [34] and is represented in Figure 8. In this work, two kinds of unit cells (BCC and BCC-Z) are analyzed under compression, with a focus on stiffness and yield stress and introducing new parameters to be taken into account during the tuning of the unit cell configuration. Indeed, the research analyzes how the mechanical properties of the unit cell can be varied changing the relative density of the structure (defined in this work as *"the actual volume occupied by the lattice structure divided by the overall volume of the structure"*, see [34] page 31) and its aspect ratio W/H (see Figure 8). For both kinds of unit cells, the research shows that the stiffness and yield stress increase when the aspect ratio W/H decreases [34]. It should be observed that when W/H decreases, also the amplitude of the angles between the struts changes. For those angles at the bottom and the top of the unit cell, this value decreases, while for those angles on the sides, this value increases (see the α angle in Figure 8). Moreover, it is worth underlying that the conclusions of Smith et al.'s study [34] are valid for BCC and BCC-Z unit cells but could be not applicable to the design

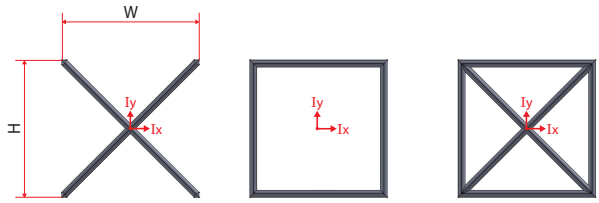

Ix	212,89 mm^4	492,00 mm^4	598,40 mm^4
Iy	212,89 mm^4	492,00 mm^4	598,40 mm^4

Fig. 9: The total area moment of inertia values (I) of the cells about centroid coordinate axes. The figure shows how 3 different geometric configurations of unit cells, having the same *W, H* and *D* values (respectively 10mm, 10mm, and 1mm), but a different struts number and arrangement, have different I values.

of other types of unit cells.

Summarizing, the design aspects to be considered for a strut-and-node based unit cell are mainly the following:

1. design or selection of the unit cell structure in terms of b and j on the basis of the desired mechanical behavior (bending or stretch-dominated, see Equations 1 and 2);
2. tuning the relative density of the cell by changing b and/or the thickness t and/or the diameter D of the struts (if the strut lenght L is kept constant);
3. tuning the *strut-and-node arrangement* considering the direction of the load (see Figure 7);
4. tuning the unit-cell geometry modifying the *amplitude of the angles* between the struts (see Figure 8), in relation to the loading conditions (direction and intensity of the load).

Finally, it should be observed that another relevant parameter that a designer could consider to create, evaluate or choose a unit cell can be its *total area moment of inertia I*, as already discussed and demonstrated in [35]. In fact, I and the moduli (e.g., Young's modulus E and shear modulus G) of the used material are responsible for the stiffness of a structure. For a given loading condition, in case of two unit cells, both bending dominated, made of the same material and with the same number of struts, but with different I values (e.g., due to a different struts positioning or D value), the one with a higher I will result as stiffer. An example, of how the total area moment of inertia I could vary, is shown in Figure 9. I determines the stiffness of a structure and, thus, affects the displacement that occurs in any direction and for every applied load. Hence, the analysis of the I value could significantly speed up the initial unit cell design and tuning in case of *bending-dominated* unit cells.

3.2 Preliminary unit cell sizing

Once the geometry of the unit cell has been identified, to guarantee its printability, the next step is to perform a proper sizing of the cell taking into account the manufacturing constraints set by the AM technology to be used according to the selected material. Examples of AM constraints to be considered are the following [15]: minimum and maximum length of the struts (L_{min} and L_{max}); minimum and maximum diameter/thickness of the struts (D_{min} and D_{max} or t_{min} and t_{max}) and the θ sloping angle (see Figure 10). These values, except θ, contribute to defining the relative density of the unit cell. On this

aspect Tanlak et al. [36] developed, for powder-bed based AM technologies, a method to predict the printable range of relative density for different unit cells, to avoid the critical radius value (for each kind of unit cell studied) i.e., the lowest and highest printable relative density to reach to prevent powder entrapment inside the inclusions of the unit cells [36]. It is important to highlight that when we refer to L_{min} and L_{max}, D and θ, we mean the values to be set to get a manufacturable cell: horizontal, vertical and sloped struts are self-supporting. This condition is necessary to avoid the support removal that, because of the characteristic scale of a MSLS (i.e., mesoscale) or of the geometry, results to be very difficult or impossible [37]. In fact, in case of AM technologies like the FDM (Fused Deposition Modeling), the supports can also be soluble and detachable without the need for mechanical removal. This kind of supports makes thus possible the cleaning of the manufactured part, but the process is not quick. With other AM technologies where it is not possible to use soluble supports, such mechanical removal is almost impossible. Hence, as underlined in [38] it is fundamental to design self-supporting lattice structures.

AM constraints are strongly related to the type of AM technology and material used [39]. It would be an error trying to use general design rules or guidelines. In fact, depending on the category of additive technology (powder-bed fusion, material extrusion, material jetting, direct energy deposition, etc.), the specific kind of technology (SLM, SLS, FDM, etc.) and the kind of material used (polymers, metals, ceramics, hybrids, etc.), the constraints linked to L_{min} and L_{max}, D and θ can be different [19, 40]. Moreover, in addition to the above-described constraints, there are some aspects, like roughness and anisotropy, which have a significant influence on the MSLS design workflow [25]. It is essential to take into account these aspects to reduce the discrepancy existing between the designed MSLS (i.e., its 3D model) and the manufactured one.

For example, roughness is the feature that has the biggest impact on the difference between the simulated mechanical properties and the real ones for a MSLS. In particular, the roughness increases determines a decrease of the moduli (E and G) and, thus, of the stiffness: the real moduli can decrease up till 68% compared to the one of its virtual model characterized by a smooth surface [41, 42]. For this reason, additively manufactured metal structures often undergo surface treatments of chemical etching, which have the purpose to reduce the roughness and to increase the structure stiffness [43]. However, a not negligible consequence of the chemical etching process is the significant thickness reduction of the diameter of the struts of the cell which can decrease up to 30% [25, 44].

Anisotropy is another aspect that has an impact on the mechanical properties of unit cells. It is due to the "layer by layer" building process and, thus, to the building direction of the 3D printed part, that determines different properties in the z direction in comparison with x and y ones [45]. In fact, according to loading condition and direction the mechanical properties of the unit cells are different. The effects of anisotropy and building orientation of additively manufactured MSLSs are discussed in more detail in [25]. The difference in term of mechanical properties for z, x, and y directions can be significant and depends on the AM technology used [25].

Tang et al. [20] studied the influence that some geometrical parameters have on the lattice structures manufacturability and, therefore, they also show the effect that the AM process has on the design workflow. Their research focused on the study of the trussed-struts, and it was based on the use of the FDM technology and the Z-ABS printing filament. These struts have been divided into two groups: horizontal and vertical (sloped). Concerning the difference between the D value of the designed struts (3D model) and the diameter of the printed ones, they discovered the following aspects. For the horizontal

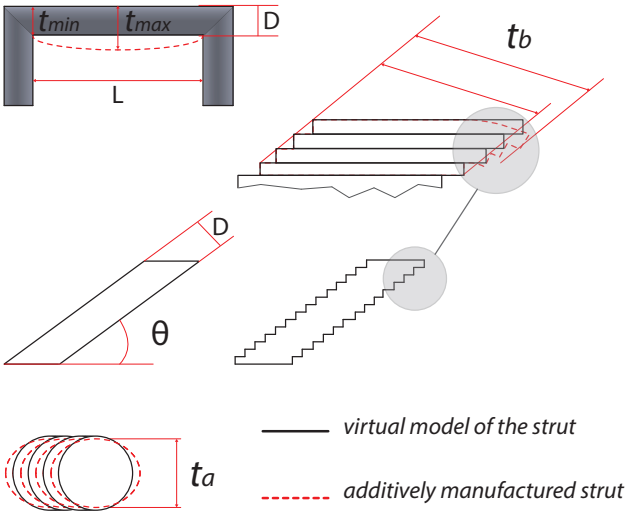

Fig. 10: The figure shows the deviation between the thickness of the virtual model of the struts (black lines) and the additively manufactured ones (dashed red lines) as discussed in [20]: both for horizontal and sloped struts such deviation is related to the change of the D value. For horizontal struts, this value can vary between t_{max} and t_{min}. For sloped struts the cross section is no more a circle but it can vary between t_a and t_b. This figure has been inspired by the work [20], pages 8 and 9.

group, the deviation is influenced by D and L (see Figure 10). For the vertical group, this deviation is influenced by θ, D and L (see Figure 10). Hence, in case of virtual struts, D coincides with the thickness t, while in case of printed struts, the thickness value and the way it varies, is influenced by the strut orientation. To mathematically describe this phenomenon, they used formulas, among which (for the complete discussion see [20]):

$$D_{\mathrm{f}} = t_{\max} - t_{\min} \tag{4}$$

$$R\mathrm{h} = \frac{Df}{D} x100\% \tag{5}$$

$$R\mathrm{s} = \left(\frac{|t_{\mathrm{b}} - D|}{D}\right) x100\% \tag{6}$$

where, D_f is the diameter variation due to the deflection, t_{max} and t_{min} are, respectively, the maximum and minimum strut

thickness in case of horizontal struts as a consequence of the deflection (see Figure 10), t_b is one of the thickness dimensions in case of sloped struts (see Figure 10). R_h (Equation 5) and R_s (Equation 6) are, respectively the *horizontal* and *sloped* deflection ratios. They can be used to check the quality of the printed structure: with values of $R_h > 25\%$ and of $R_s < 10\%$ the stringing of the struts occurs [20].

For the horizontal group, the study was based on 30 samples. They discovered that the t_{max} value is mainly due to the gravity, the viscosity of the material, the D and L values. For the vertical group, the samples used were 45. The t_a and t_b values are a consequence of the gravity, the viscosity of the material, θ, D and L values. When θ is low, the length of the *cantilever* produced by consecutive and overlapping layers becomes higher, and it more significantly affects the dimensional deviation between the thickness of the 3D model, and one of the manufactured struts (see Figure 10).

To conclude, performing a proper dimensional sizing of the cell means appropriately taking into account both the specific AM constraints (given by the AM technology and the material used) but also other aspects already discussed in the literature (e.g., R_h and R_s ratio, see [20]). They all concur to determine the overall quality of the unit cell and thus, of the resulting structure.

Summarizing, the evaluation of AM constraints helps to define the following parameters:

1. the L_{min} and L_{max} values of the struts;
2. D_{min} and D_{max} (or t_{min} and t_{max}) of the struts (see Figure 10);
3. the θ sloping angle (see Figure 10).

3.3 Population of the design space

Once the unit cell has been identified, and its preliminary sizing has been performed, the next phase of the process consists in creating the MSLS, i.e., populating the design space.

As anticipated in Section 2, there are two population strategies, named uniform and conformal. In the first case, the array of unit cells follows a periodic distribution (in *x, y, z*) and, thus, the unit cells are arranged according to regular and fixed distances. As shown in Figure 11, the uniform population is based on an absolute logic distribution, which is not influenced by the design space geometry [46]. When a uniform population of the design space is performed, the management of the boundaries is accidental and the surfaces of the design space act as cutting surfaces for all the struts of the unit cells placed at its boundary. Uniform MSLSs have the advantage that all unit cells have the same dimension and shape; on the other hand, the integrity of the unit cells geometry, at the boundary, cannot be guaranteed (see Figure 11). This fact might generate poorly connected areas [20].

Vongbunyong and Kara [47] proposed a method, defined as P-HGM (Prefabrication Hybrid Geometric Modeling) for a rapid generation of uniform MSLSs. Their method can be adopted for symmetrical unit cells built using surface modeling software tools, and not solid modeling ones. According to this method, the unit cells are trimmed through the use of a bounding box, without the need of boolean operations: the struts are sectioned, and the edges that lie on the bounding box are automatically removed. This method allows controlling the connections between the unit cells: it avoids overlapped faces and problems related to the mapping of the normals (when generating the ".STL" file), and it ensures better and more

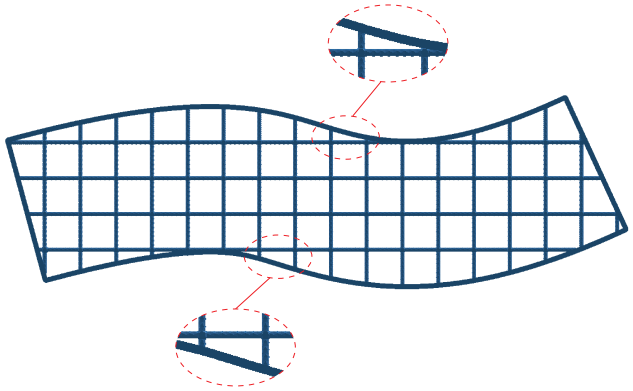

Fig. 11: The uniform population is based on a periodic unit cell distribution. The figure shows how all unit cells have the same shape and dimensions. Dashed red lines are used to highlight that the unit cells integrity, at the boundary, is accidental.

uniform management of the strut diameter at the joints. It should be underlined that surface modeling software tools give the possibility to replace boolean operations with trimming one. Boolean operations involve two solids that can be joint, intersected or subtracted. Trimming operations work on surface meshes (planes, faces, etc.) and simply cuts a surface using another one. Replacing the use of boolean operations with trimming ones, time and computational resources can be significantly reduced [47].

When the population is performed applying a conformal distribution (see Figure 12), the geometry of the unit cells is modified to enable a conformal mapping of these within the design space. In [48] an algorithm is described to generate a conformal hexahedral mesh of the design space that will be used to control the unit cells arrangement. This algorithm makes use of offset surfaces that are generated starting from the splitting of the external surfaces of the design space into multiple *relatively flat regions* (as defined in [48]). Loft operations are performed to connect these surfaces and to identify volumes that will be then divided into hexahedra: they represent the spaces where the unit cells will be placed. To guarantee the success of this operation, it is fundamental that both the two surfaces are parametrized.

With a conformal population, the management of the unit cell positioning occurs through an approach that has a more in-depth control of the design space boundaries compared to the uniform population and, thus, the integrity of all unit cells is retained. For this reason, conformal population can be considered a better approach when one of the functional targets set for the MSLS (see Figure 3) is the stiffness [4]. Nevertheless, sometimes it can happen that a manual relocation of some joints, not wholly conform to the boundaries, could be needed [3]. Looking at Figure 12, it should be observed that with a conformal population not all the unit cells have same dimensions and shape (they are changed to guarantee conformity at the boundaries). This aspect sometimes can be significantly in contrast with some manufacturing constraints, like minimum and maximum length of the struts, sloping angle and diameter/thickness of the struts (see also Section 3.2). Furthermore, conformal population is often applied to simple geometries since it is not an easy task to be performed in case of reasonably complex geometries, as already underlined in [20].

Alternative methods to uniform and conformal population have been proposed by Tang and Zhao [49], Reinhart and Teufelhart [50], Wu et al. [51] and Kolken et al. [52]. Tang and Zhao [49] proposed a method where the design space is

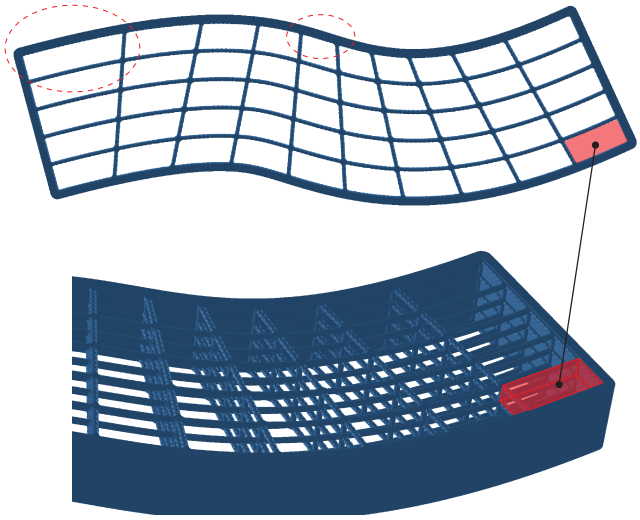

Fig. 12: The conformal population is based on a distribution of the unit cells that is conformal to the boundaries of the design space. The figure shows that the unit cells do not have the same shape and dimensions. The dashed red lines and the red box highlight that they are fully conformal to the boundaries and their integrity is preserved.

divided into FVs (Functional Volumes) and FSs (Functional Surfaces). The unit cell orientation and, in particular, the degree of rotation of the unit cell within the functional volume is defined according to the loading conditions and the constraints. The functional surfaces, instead, work as connections between the different functional volumes. The final result obtained by using this method is a design space populated by different functional volumes, where each one has a different orientation: the objective is to optimize the structural performance of the structure according to the global loading conditions and constraints [49]. Reinhart and Teufelhart [50], instead, go beyond the concept of population based on an array of unit cells. They describe a case study where the population starts calculating the flux of force of a design space, after the definition of the load and constraint conditions. Finally, they define the orientation and shape of the single struts, building the same struts along the flux of force, in relation to the main stress tensors [50]. Wu et al. [51] starting from an adaptive rhombic grid and the aim of generating self-supporting infill structures, through the use of efficient FEM simulation and topology optimization of millions of finite elements, demonstrated the validity of a hierarchical infill generation approach to optimize the mechanical stiffness and static stability of the structure. This hierarchical optimization approach of Wu et al. [51] is based on the idea that, splitting a cell into multiple items, allows improving its mechanical stiffness since it increases the quantity of material. Besides, choosing not a uniform but an adaptive cells subdivision of the infill structure also allows optimizing the position of the center of gravity of the object to be printed [51]. Kolken et al. [52], instead, developed an innovative concept of the population of the design space based on a hybrid distribution of unit cells. They used a combination of negative and positive Poisson's ratio unit cells to improve and maximize implant-bone contact when the implant undergoes biomechanical loading [52].

To conclude this Section, it is further emphasized that the population phase has the role of generating homogeneous MSLSs and that various software can support the designer in performing this activity, especially for what concerns the generation of conformal structures.

3.4 Setting of the MSLS density gradient

Once the homogeneous MSLS has been created, the next phase consists in finalizing the relative density of the structure. To change this value we have two approaches which are associated with the thickness or diameter of the struts of the cells. The density gradient of a MSLS, in fact, can be homogeneous or heterogeneous. With homogeneous density gradients, the diameter of the struts does not locally change [53]. This means that all the struts of the cells are simultaneously varied. When heterogeneous density gradients are used, the approach is to correlate the density and, therefore, the diameter/thickness sizing of the struts to the loading conditions. An example of an application of a heterogeneous gradient is represented in Figure 13. This figure takes as reference the works described in [54, 55].

Many studies have been done on the application of heterogeneous density gradients and there are software applications embedding specific commands to address this phase. New methods focused on improving this phase of the process have also been developed. For example, Nguyen et al. [3], developed a method called SMS (Size Matching and Scaling). This method is based on the principle that the stress distribution for MSLSs is similar to that of a fully solid material having the same external volume. Based on this assumption and on the distribution of the local stresses detected using Finite Element Analysis (FEA), the unit cells are sized. This sizing is performed through mathematical equations that calculate the D_{max} and D_{min} values of the struts. The main steps of the SMS method are the following: FEA on the fully solid geometry; mapping and normalization of the stress on the MSLS; D_{max} and D_{min} definition [3].

Another method is based on models made of voxels. The model is a 3D matrix (made of different cubic volumes, known as voxels) that defines the entire volume of the design space similar to what the pixels do with a 2D image. One of the easiest approaches used for voxel method gives to any voxel a value between 0 and 1, where 1 means a solid space, and 0 a void one. Based on this principle and overlapping a grey scale image on the volume made of voxels (considering the ”black” as solid and the ”white” as an empty space), the method can be used to build functionally graded MSLSs. Through this approach, maps, referred to stress distribution obtained setting the mechanical constraints and the loading conditions, can be used [22]. Applications, aimed to create functionally graded densities, based on grey scale (see Figure 13) or dithering images have been performed by Brackett et al. [56]. The dithering is a method based on the use of images where the gradient of density is created by using the *dot* as the basic element. The image to be superimposed on the MSLS is composed of an array of dots. The density of the dots within the image boundaries can vary, and it depends on the amount of load to bear. Once the dots are connected to the MSLS to be functionally graded, where the amount of dots is higher, the diameter of the struts is increased and thus, accordingly, the relative density of the MSLS. Where the amount of dots is lower, the diameter of the struts is decreased and, therefore, the relative density as well [23, 56].

The output of this fourth phase of the design process (Figure 3) is a MSLS having the desired relative density.

3.5 Verification and optimization of the MSLS

3.5.1 Verification of the MSLS behavior

The last step of the design workflow (see Figure 3) is the verification of the MSLS behavior through simulation tools. These tools can be used both to evaluate and develop the MSLS. Indeed, some of the methods described in the previous

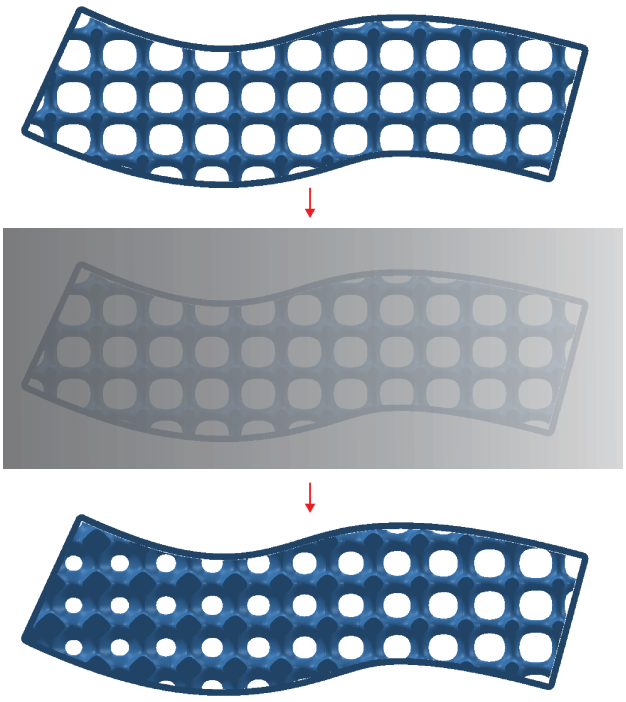

Fig. 13: The figure shows the application of a heterogeneous gradient through the use of a grey scale image that is overlaid to a uniform lattice structure. The darker areas have a higher relative density (through the struts thickening), while the clearer ones have a lower relative density. Both the uniform and graded structures were modeled using the software, developed at the University of Nottingham, mentioned in [14].

sections make use of simulations, for example, to create and optimize the geometry of the unit cells (Section 3.1), and their density gradients (Section 3.4). However, the primary task of simulation tools is to predict and evaluate the mechanical behavior of a single unit cell or, of the entire MSLS [57]. A reference on this topic is the review analysis performed by Dong et al. [25]. This review gives a clear and in-depth overview of the main methods used to simulate and predict the mechanical behavior of lattice structures, highlighting advantages and disadvantages for each method. The discussion provided in this Section has been inspired by this review.

The most used methods are homogenization method, FEA based on beams, and FEA based on solid elements.

The *homogenization method* is a mathematical approach that replaces the geometry of the MSLS with the one of an equivalent (in terms of mechanical properties), fully dense material. This method has low computational costs, but also some considerable limits. In fact, it cannot be applied to MSLSs based on heterogeneous density gradients, and it is not easy to manage in case of complex geometries [39, 58]. Conversely, FEA based on beams or solid elements are easier to manage and can be applied to reasonably complex shapes [25].

FEA on beams has a moderate computational cost and can be used for MSLSs with heterogeneous density gradients (it cannot be done with homogenization). Its limits are the following: difficulty in providing accurate results when the struts are not thin enough; poor capability in predicting the stress distribution that occurs at the struts joints [25]. One way suggested in the literature to decrease the effect of this limit is to increase the thickness of the joints. Labeas and Sunaric [59], for example, demonstrate that for a MSLS with BCC unit cells a 40% increase of the strut cross-section in the nodal regions

is suitable to give results very close to those of the experimental tests, predicting in detail the mechanical behavior of the MSLS [59].

FEA on solid elements, instead, is more suitable to manage higher diameters or thicknesses and to accurately predict stress distribution in the nodal areas between the struts. Moreover, it provides the possibility to perform simulations on the as-fabricated MSLS, incorporating the defects due to the manufacturing process, using image-based FEA techniques [25,60,61]. This possibility helps to reduce the gap existing between the simulated and the real behavior of a MSLS, taking into account the influence of the AM process. Image-based FEA, in fact, are performed adding to the virtual model the defects, observed on the manufactured part, that are consequences of the selected AM technology, the material, and the process parameters. The primary limit of FEA on solid elements is linked to computational costs and time [25].

Many studies have been done on the simulations of MSLSs. Ushijima et al. [62] used FEA to investigate the compressive behavior of lattice structures made of stainless steel and manufactured using the SLM technology; they showed that there is a good match between experimental results and the simulation for lattice structures having a low relative density [62].

Smith et al. [34] performed a study on the compressive behavior of two kinds of unit cells, manufactured using the SLM technology, named BCC and BCC-Z (see Figure 14). They focused on parameters like stiffness and yield stress, using FEA based on solid elements and beams. In particular, the authors investigated how the relative density and aspect ratio (W/H, see Figure 8) affect the stiffness and the yield stress of the cell. They used, for each unit cell, four samples with a different relative density and aspect ratio. For FEA on the solid elements they used struts wholly straight and with a constant diameter; the compression test was simulated by applying the same loading conditions (for both cells) and using a fixed rigid plate where to crush the unit cells progressively (see Figure 14). For FEA on beams, the approach is similar, and the adjustment, suggested by Labeas [59] has been used, i.e., the increase of the cell thickness in the nodal regions, to better calculate their stress and strain distributions. Finally, they compared the results (stress/strain curves) obtained by FEA on the solid elements, by FEA on beams and the experimental results of the compressive tests carried out on the samples manufactured using the Selective Laser Melting (SLM) technology. With FEA on beams, the phenomenon of densification is not taken into account, since this approach does not allow managing the contact between individual struts.

The results of their study show that for BCC unit cells there is a 15% difference between the values of the initial stiffness of the FEA based on solid elements and also of the FEA on beams with respect to the experimental results. For the BCC-Z unit cell, the approximation is 5% for the FEA on beams and 30% for the FEA on the solid elements. In this case, there is an overestimation that could be due to the presence of the vertical strut in the middle of the cell (see Figure 14, right). This vertical strut creates a thickening in the same nodal region that affects the data accuracy [34]. In general, as proven by Ushijima et al. [62], all the simulations show a high adherence to the experimental tests but for MSLSs having a low relative density.

Smith et al. [34] in their study, as shown in Figure 15, also apply the FEA on arrays of unit cells, demonstrating that, with more regular geometries (i.e., BCC unit cell), the analysis on one individual unit cell can be sufficient to predict the mechanical response of the MSLS. Otherwise, for arrays of unit cells less regular (i.e., BCC-Z unit cell), an approach that evaluates the entire MSLS using multiple unit cell models and not only one individual unit cell, can be necessary because

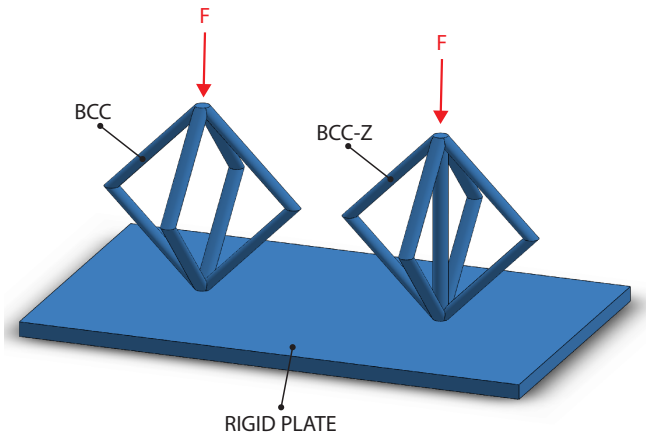

Fig. 14: The figure shows the model that has been used in [34] for performing a FEA on BCC and BCC-Z unit cells. The solid model is based on the use of struts wholly straight and with a constant diameter. A compression test is simulated applying the same loading conditions on the planar face at the top of each unit cell and using a rigid plate to crush the same unit cells progressively.

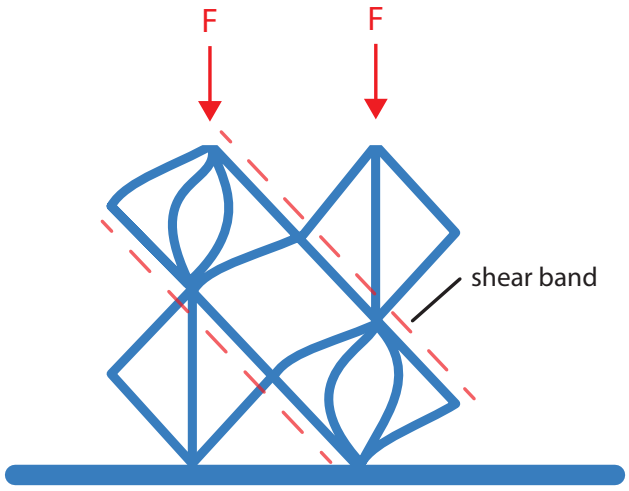

Fig. 15: The figure shows how shear bands (dashed red lines) can occur when an array of unit cells less regular, like BCC-Z with the characteristic vertical strut in the middle, is loaded (see also Figure 14). In these cases, a simulation performed on a single unit cell can be not sufficient to get information on the deformability of a lattice structure. This image has been inspired by the work [34], page 39.

the behavior under a load is not uniform and local failures or shear bands can occur [34].

To conclude, in this Section the following two main aspects have been addressed. First, it has been discussed how simulation tools can be considered as valid support for the MSLSs design process. However, it is essential to be aware of the limitations related to the accuracy of the prediction of their mechanical behavior, and the computational effort needed, to choose the most suitable approach/strategy. In particular, an important aspect is to identify a right balance between the computational effort required and the desired accuracy according to the specific aim of the simulation. For further details about advantages and disadvantages of the various simulations methods, the work of Dong et al. [25] is suggested.

Second, it has also been discussed the mismatch between the physical model of a MSLS and its virtual replica. This mismatch is referred to mechanical behavior, dimensional deviations and manufacturing defects [63, 64]. This fact suggests

the actions to be undertaken, starting from the necessity to continue the creation of a strong awareness about the issues to be faced, and the decision to be made when designing MSLSs. Hence, simulation tools should provide features that can predict the mismatch mentioned above. According to the specific AM technology and material used, simulations should give insights on the dimensional deviations, and manufacturing defects, which are responsible for the different mechanical behavior observed comparing the results of the FEA, and the experimental ones retrieved from the physical model [65].

3.5.2 Optimization of the MSLS structure

The topology optimization is based on algorithms aimed to use the material where needed and to find its optimal distribution [4]. Optimization algorithms can be of great help when designing lattice structures (see also Section 3.3), even if some issues still need to be faced among which, as already discussed in [66], the importance of including manufacturing constraints in the design process. The research community has also started addressing this challenge, as demonstrated in the work of [51] discussed in Section 3.3 or, in the works cited in this Section. Indeed, manufacturing constraints are instead fundamental to guarantee the efficiency and the feasibility of the printing process (see also Section 3.2 and Figure 3). Many relevant studies are already available in the literature demonstrating how topology optimizations results can be used efficiently as input for generating lattice structures having improved characteristics, in particular in term of stiffness. The aspect to be underlined that will also be recalled in Section 3.6 is that topology optimization allows generating both the geometry of the cell and the structure. Hence, studies related to topology optimization could involve nearly all phases of the design process represented in Figure 3. Even if this approach has been placed at the end of the design workflow, actually, it can be of help also for the previous phases.

For example, Wang et al. [67] proposed a method, also based on the results discussed in [68] for the multiscale topology optimization of additively manufactured graded lattice structures. Their method is based firstly on the optimization of the geometry of the global structure and its mesostructures, secondly on the optimization of the distribution of the mesostructures through the application of a density gradient. To demonstrate the method effectiveness they developed and tested optimized cantilever beams [67]. The results demonstrated a superior stiffness for the optimized graded lattice structure compared to the baseline design with uniform mesostructures [67]. Conversely, the work of Alexandersen and Lazarov [69] aims at overcoming the limitations of homogenization-based multiscale optimization methods, which do not efficiently manage microstructural details. Hence, a computationally efficient approach is described to optimize the macroscopic response of the structure from the analysis of the localized behavior of the structure which allows optimizing its microstructural details. Hence, this method provides also the benefit of generating manufacturable microstructures tailored for specific applications [69]. Wu et al. [70], instead, developed a voxel-based optimization method, to generate porous infill structures able to mimic the ones of bones. Their method imposes constraints on volume fractions to regulate the local material distribution in a given design domain, under external and specific loading conditions. They also demonstrated that the generated bone-like porous structure is stiffer than optimized rhombic ones. This approach is aimed to take into account, during the optimization process, also the manufacturing constraints (e.g., minimum feature size) associated with the AM technology (Selective Laser Sintering) used in their study [70].

To conclude, it is worth underlying that, this focus on topology optimization methods, developed and applied in the AM field, does not aim to provide a complete review on the topic, but rather to underline the following aspects. First, topology optimization methods can be seen also as strategies for generating lattice structures characterized by complex geometric models (see also Section 3.6). Second, the development of such complex geometries must include manufacturing constraints to guarantee their printability. Third, considering the ”punctual” control of the material distribution allowed by AM technologies, methods to optimize the structure locally, are very promising.

3.6 The modeling phase of MSLSs

After having described the design phases (Figure 3), this Section addresses the main aspects dealing with the modeling phase of MSLSs. Dedicated software tools supporting the generation of the 3D model of MSLSs are already available on the market. A list of these tools is provided in [71] and [72]. Since the software market is evolving rapidly, rather than providing an overview of the main characteristics of these tools, which can become quickly outdated, this Section focuses on the different modeling strategies that can be used.

The main strategies nowadays applied are summarized in the work of Tao and Leu [4]. They classify them as *primitive based*, *implicit surface based* and *topology optimization based*. Topology optimization strategies are not analyzed here since they have been already discussed in Section 3.5.2.

The *primitive based* strategy builds the unit cells applying boolean operations to simple geometric primitives, like cubes or spheres. The modeling activity can be performed using 3D CAD software tools: parametric models of the MSLS can be generated and easily modified. The disadvantage is related to the dimensions of the files. As already underlined in [73], managing complex structures is quite challenging since a high number of boolean operations could be needed, and also a high number of surfaces has to be managed [74]. Obviously, this is true unless dedicated modules are integrated with current 3D CAD software tools. An interesting example related to the development of a CAD-based tool to support the 3D modeling of MSLSs is described in [75].

The *implicit surfaces based* strategy is related to tools that make use of implicit mathematical equations to parametrically manage the dimensions of the structure, of the struts and their fillet at joints [4]. Functionalities of this kind have been developed, also for 3D printing mathematical functions for educational purposes (e.g., see [76]). Nowadays they are of great help for 3D printing structures such as the TPMSs (see also Sections 1 and 3.1). An example related to the use of implicit formulations is presented in [73].

A further interesting classification of modeling strategies used for representing cellular structures is provided in [77]. In this paper, modeling strategies are classified into two main groups on the basis of the approach used for representing the 3D model, i.e., Boundary representation (BRep) or Volume representation (VRep). Finally, to overcome the limitation of primitive-based strategies, to optimize the computational efforts required, and to avoid the generation of non-manifold geometries an innovative mesh-based modeling approach is described in [78].

To conclude this Section, the following aspects are highlighted. As shown in Figure 3, the design process of MSLSs is characterized by a high number of redesign cycles. This is due to the complexity of the design activity to be performed

since geometrical and technological aspects are strongly correlated. Also, we have to consider that the knowledge related to the design of MSLSs is still mainly at a research-level and further examples and application cases are needed to retrieve the insights necessary to guide designer's decisions better. This lack of knowledge is also responsible for these redesign cycles. Hence, software tools should allow an easy update and change of the MSLSs geometry, the possibility to assign manufacturing constraints and to check their fulfillment automatically. Moreover, although software tools having libraries of predefined unit cells are already available, however, classifying these cells considering their mechanical behavior (e.g., *stretch-dominated* or *bending-dominated*) could be, for example, relevant piece of information upon which starting the design phase.

4 Discussion

The analysis of the literature provided in Section 3, has highlighted the main phases to be performed and issues to be faced when designing MSLSs. This Section will be instead dedicated to the starting point of the design process, i.e., the setting of the functional targets to reach. Indeed, nowadays, such functional targets are mostly focused on searching for the optimal stiffness to weight ratio when designing lightweight solutions. The fulfillment of this target is made possible by AM technologies, which allow a local and punctual control of the material distribution within the design space. However, this is a too narrow view of the functionalities that these structures could provide. The aim of this Section is thus to expand this view providing an overview of both advanced and emerging functionalities of MSLSs: the intent is to explore the *design for functionality* concept (as defined in [79]).

The most widespread applications of MSLSs are referred to biomedical, aerospace and automotive (mainly racing) fields [4]. It is evident that in these fields, the possibility to simultaneously develop stiff and light solutions can give considerable advantages. For example, in the biomedical field, lightweight is necessary to build implants (mainly in titanium alloys) with a weight similar to that of the replaced bone, and a degree of porosity suitable to promote the proliferation of the living cells (e.g., see [80–85]). In the aerospace and automotive fields, a weight decrease can mean better performances with less fuel consumption (e.g., see [4, 83]). Hence, if, on the one hand, the lightweight functionality, in term of reduction of material resources is the driver of the diffusion of MSLSs applications [86], it cannot be considered as the only design target to be pursued. Other functionalities, instead, can be experimented and must be explored.

For example, the fields of applications described in [6] for metal foams can be valid also for bending-dominated MSLSs (see also Section 3.2). Indeed, functionalities concerning heat exchange and acoustic insulation capabilities have been already tested [87]: the high area to volume ratio, on the one hand, and the high number of internal voids, on the other, can significantly increase the heat exchange capabilities and insulation efficiency of a system. A further relevant application, concerning the heat transfer capabilities of these structures, is related to the design and manufacturing of *conformal cooling channels*, as demonstrated in [88]. However, it is evident that the substitution of metal foam with more expensive MSLSs, from the manufacturing point of view, can be justified considering the design freedom provided by AM technologies.

The stiffness of both *stretch-dominated* and *bending-dominated* MSLSs can be tuned and modulated, for example along the different loading directions, as discussed in Section 3.1. This kind of structures can be then used also for energy absorbing

applications, e.g., as discussed in [21, 89]. Another interesting and innovative application of MSLSs is in the filtering field as demonstrated in [90], and as already discussed in [4]. In this case, the benefit is obtained by combining the possibility to have a high number of voids with the possibility to orient them to reduce pressure drops.

Together with its lightweight capability, the further functionalities provided by these open struts-based structures (e.g., improved heat exchange, acoustic, damping and ventilation capabilities) has pushed their use into sandwich panels (e.g., see [91–93]) as alternatives to the well-known honeycomb structures. This fact has pushed the research community on also exploring the shear behavior of cellular structures (e.g., see [91–96]). Indeed, as explained in [94], when the panel undergoes a bending load, it is the shear response of the core which determines its flexural strength. However, the strut-based structures analyzed in these studies have been obtained mainly using conventional manufacturing processes, except in [93] where an investigation of the shear response of a structure, manufactured using the SLM technology, is provided. Hence, further research efforts are needed to continue the exploration of the shear behavior of MSLSs.

When discussing the potential functionalities of MSLSs, it is necessary to distinguish those that can be considered as advanced, and that can be developed at an R&D level (like the previous ones), from those that can be considered as emerging. In this second case, new functionalities of MSLSs are discovered "playing" not only with the structure geometry but also with the material and the building process. An overview of works describing such emerging functionalities is presented below. Before starting this overview, however, it is worth underlying that the objective of these works is to explore new potentialities of lattice structures and/or to develop innovative unit cells. Hence their focus is more on the outputs of their theoretical and/or experimental studies, rather than on deriving a structured design method.

A first relevant example is represented by the possibility of transforming these structures into mechanisms, i.e., the so-called *metamaterial mechanisms* as described in [97]. In this application, a component can be seen as the sum of multiple MSLSs, each one having its mechanical behavior (e.g., stiff or soft). Hence, selecting the proper material, a unique component can be used to generate a mechanism made up of different elements (e.g., in [97] several examples are provided among which a door mechanism built as a unique component). To select the proper cell arrangement, with respect to the desired mechanism, a dedicated software application has been developed combining a graphical editor and a simulation environment: it is the feedback provided by the simulation (see also phase 5 in Figure 3) which drives the user towards the selection of the right unit cell and structure.

A second example is represented by *auxetic MSLSs*. They are characterized by a negative Poisson's ratio: under uniaxial compression, they shrink laterally, or under uniaxial tension, they enlarge laterally. They can be classified as a mechanical metamaterial [98]. 3D auxetic lattice structures, because of their particular stress distribution, and their capability to change their geometric configuration, can be used for a wide range of applications such as fasteners, textiles for medical applications, protective clothing, etc. [99, 100]. For example, Li et al. [100] discussed an approach to design 3D auxetic lattice structures able to generate out-of-plane deformations through the use of curved struts. The curved shape of the struts (called *ligaments* by Li et al. in their study) and their arrangement are responsible for the auxetic behavior. The so-called *"out-of-plane"* deformation is different by the *"in-plane"* one that is typical of 2D auxetic structures, which are currently the most explored structures since they are easier to design and print. This example shows how new functionalities can be explored working on

the design of the unit cell, and specifically, of its struts. Hence, works as one of Li et al. [100] are focused on expanding the range of choices related to the first phase of the design process which is the *"Unit cell design or selection"* (see Figure 3).

A third example, is represented by *4D materials* (e.g., see [101] for a review). Studies addressing this topic, combine the design freedom given by the AM process, with the modularity of lattice structures and the additional functionalities provided by the so-called smart materials, i.e., materials capable of changing their properties or shape in response to external stimuli (e.g., temperature, electric or magnetic field, mechanical loading conditions, etc.) [102]. In this case, the material plays a fundamental role in determining the new functionalities of the structure. 4D materials can be used for auxetic, deployable or self-assembly structures and are promising for fields of application like the aerospace and biomedical ones. For these fields, mechanical or electromechanical stimuli are not always applicable, and the change of shape cannot be manually achieved [4, 103]. The smart materials mostly used for 4D materials are SMAs (Shape Memory Alloys), SMPs (Shape Memory Polymers) and hydrogels [104–106]. The first two use a thermal stimulus to trigger the change of the shape while hydrogels are activated by the humidity. They change shape (by swelling) reacting to the presence of fluid in their environment. Wagner et al. [106] presented a work where an auxetic lattice structure was manufactured using a single material and, in particular, an SMP. The combination of the mechanical behavior given by the auxetic lattice structure with the SMP capabilities allowed a significant change of the structure shape. They measured a 200% change of the area enclosed by the structure [106]. In case of *4D materials* the further level of complexity in the design of the MSLS is given by the multiple functional targets to be fulfilled.

A fourth example is represented by *soft and highly-stretchable metamaterials*. They combine the 3D free-form given by additively manufactured lattice structures with the high stretchability of materials like elastomers. Again, also, in this case, the material plays a fundamental role in determining the new functionalities of the structure. These kinds of metamaterials can be used for a wide range of applications including soft robotic, packaging for energy absorption, rehabilitation devices, soft and wearable electronics [107, 108]. All these applications take advantage of the high stretchability and the dampening properties of these metamaterials. For robotic applications they are used as connectors to bridge parts where bending or rotation is required; in packaging applications, they could be used as dampers to shield impacts while, for rehabilitation devices, they could be used to support the movements of the joint to rehabilitate. Finally, in case of soft and wearable electronics, they can act as flexible supports for building integrated electronic solutions. Jang and Wang [108] presented a method to fabricate highly-stretchable lattice structures. They use a process where a hollow and water-soluble lattice structure is built using micro-stereolithography. This structure is used as a scaffold to cast (using a syringe) the catalyzed elastomer. Once the elastomer is cured, the scaffold is dissolved in a water solution. The metamaterial fabricated using this method is characterized by lightweight and an ultrahigh and reversible stretchability. It can strain up to 414% [108].

From this overview, the following couple of considerations can be drawn. Again, as already underlined in Section 3.6, considering the complexity and the novelty that characterize MSLSs, there is the need of tools tailored to their design process as well as of more case studies to build a solid background on the topic. In addition, as the new emerging applications demonstrate, such process will become even more "multi-disciplinary" since multiple aspects (i.e., geometry, material, process) will concur in "shaping" MSLSs functionalities. Hence, to foster the exploitation of such emerging functionalities into

real applications, a further level of development of their design process, and of its supporting tools, is required.

5 Conclusions

Considering the growing interest of both the research and industrial communities, in the design and manufacturing of non-stochastic cellular structures (thanks to the extensive diffusion and rapid development of AM technologies), this paper proposes an overview of the design process of these structures. The discussion is focused on additively manufactured Meso-Scale Lattice Structures (MSLSs). These are structures whose unit cell dimensions vary from 0.1 to 10.0 mm. Specifically, we concentrate on MSLSs characterized by a strut-and-node architecture. Even if most of the examples provided are focused on this kind of structure, however, the described design process is valid also for other types of cellular structures, such as, for example, the TPMS (Triply Periodic Minimal Surface). The intent of focusing the discussion on this kind of structures is given by the design freedom that strut-and-node based structures can offer.

The contribution of this review is twofold: providing a comprehensive view of the lattice structure design process and of the design strategies currently available, which is still lacking; providing an attempt in uniforming the technical terms used when describing the lattice structures design process. Five main phases have been identified, starting from the *"Unit cell design or selection"* until the *"Verification and optimization of the MSLS"*. The final part of the analysis is also dedicated to the review of the full range of functionalities that these structures can provide.

From the literature analysis, it comes out that further researches are needed, and in particular:

1. case studies describing the process followed to develop the MSLSs, to deepen the knowledge of MSLSs design;
2. strategies/approaches to forecasting the mismatch existing between the designed MSLS and the manufactured one, to allow designers to prevent the influence of the manufacturing process on MSLSs;
3. optimization/population/gradient-based strategies able to locally control the material distribution to develop MSLSs with enhanced and customized properties to take advantage of the "punctual" control allowed by AM technologies;
4. optimized modeling strategies of MSLSs to reduce the computational efforts required when generating complex geometric structures to exploit the design freedom offered by AM technologies fully;
5. integrated design tools able to reduce ineffective redesign cycles by allowing the designer approaching the design problem from a multidisciplinary perspective, i.e., by simultaneously taking into account technological, geometrical and technical requirements;
6. development of new functionalities/properties that go beyond lightweight, through advanced approaches integrating MSLSs design, materials, and manufacturing technologies.

Three are the main figures that may benefit from this review: designers, software developers, and researchers. Designers can retrieve insights on: the design phases to be carried out; the design possibilities offered by these structures; the influence of the manufacturing process on design choices; potentialities and limits of current modeling and simulation tools. Software developers could get a more precise understanding of: the design process as a whole; how much decisions, taken at each level of the process, influence the quality of the 3D printed object; the potentialities and limits of current modeling and simulation

tools. Finally, researchers could use this review as a starting point for addressing the identified open issues or exploring new and advanced functionalities of lattice structures.

References

[1] Ashby, M., 2006. "The properties of foams and lattices". *Philosophical Transactions of the Royal Society of London A: Mathematical, Physical and Engineering Sciences,* **364**(1838), pp. 15–30.

[2] Hearn, G., and Adams, E., 2006. "Shape selection for lattice structures". *Journal of Structural Engineering,* **132**(11), pp. 1713–1720.

[3] Nguyen, J., Park, S., Rosen, D. W., Folgar, L., and Williams, J., 2012. "Conformal lattice structure design and fabrication". In Solid Freeform Fabrication Symposium, Austin, TX, pp. 138–161.

[4] Tao, W., and Leu, M. C., 2016. "Design of lattice structure for additive manufacturing". In Flexible Automation (ISFA), International Symposium on, IEEE, pp. 325–332.

[5] Miyoshi, T., Itoh, M., Akiyama, S., and Kitahara, A., 2000. "Alporas aluminum foam: production process, properties, and applications". *Advanced engineering materials,* **2**(4), pp. 179–183.

[6] Ashby, M. F., Evans, T., Fleck, N. A., Hutchinson, J., Wadley, H., and Gibson, L., 2000. *Metal foams: a design guide*. Elsevier.

[7] Aurenhammer, F., 1991. "Voronoi diagrams—a survey of a fundamental geometric data structure". *ACM Computing Surveys (CSUR),* **23**(3), pp. 345–405.

[8] Nowak, A., 2015. "Application of voronoi diagrams in contemporary architecture and town planning". *Challenges of Modern Technology,* **6**(2), pp. 30–34.

[9] Tonelli, D., Pietroni, N., Puppo, E., Froli, M., Cignoni, P., Amendola, G., and Scopigno, R., 2016. "Stability of statics aware voronoi grid-shells". *Engineering Structures,* **116**, pp. 70–82.

[10] Michielsen, K., and Stavenga, D. G., 2008. "Gyroid cuticular structures in butterfly wing scales: biological photonic crystals". *Journal of The Royal Society Interface,* **5**(18), pp. 85–94.

[11] Jung, Y., and Torquato, S., 2005. "Fluid permeabilities of triply periodic minimal surfaces". *Physical Review E,* **72**(5), p. 056319.

[12] Hoare, S. H. N., and Murphy, D. T., 2012. "Simulation of acoustic wave propagation in 3-d sonic crystals based on triply periodic minimal surfaces". In Baltic Nordic Acoustics Meeting (BNAM2012), York.

[13] Abueidda, D. W., Bakir, M., Al-Rub, R. K. A., Bergström, J. S., Sobh, N. A., and Jasiuk, I., 2017. "Mechanical properties of 3d printed polymeric cellular materials with triply periodic minimal surface architectures". *Materials & Design,* **122**, pp. 255 – 267.

[14] Maskery, I., Sturm, L., Aremu, A., Panesar, A., Williams, C., Tuck, C., Wildman, R., Ashcroft, I., and Hague, R., 2017. "Insights into the mechanical properties of several triply periodic minimal surface lattice structures made by polymer additive manufacturing". *Polymer,* **In Press**.

[15] Thompson, M. K., Moroni, G., Vaneker, T., Fadel, G., Campbell, R. I., Gibson, I., Bernard, A., Schulz, J., Graf, P.,

Ahuja, B., and Martina, F., 2016. "Design for additive manufacturing: Trends, opportunities, considerations, and constraints". *CIRP Annals,* **65**(2), pp. 737 – 760.

[16] Ozbolat, I. T., and Khoda, A., 2014. "Design of a new parametric path plan for additive manufacturing of hollow porous structures with functionally graded materials". *Journal of Computing and Information Science in Engineering,* **14**(4), p. 041005.

[17] Chu, C., Graf, G., and Rosen, D. W., 2008. "Design for additive manufacturing of cellular structures". *Computer-Aided Design and Applications,* **5**(5), pp. 686–696.

[18] Deshpande, V., Ashby, M., and Fleck, N., 2001. "Foam topology: bending versus stretching dominated architectures". *Acta materialia,* **49**(6), pp. 1035–1040.

[19] Kranz, J., Herzog, D., and Emmelmann, C., 2015. "Design guidelines for laser additive manufacturing of lightweight structures in tial6v4". *Journal of Laser Applications,* **27**(S1), p. S14001.

[20] Tang, Y., Dong, G., Zhou, Q., and Zhao, Y. F., 2017. "Lattice structure design and optimization with additive manufacturing constraints". *IEEE Transactions on Automation Science and Engineering*, pp. 1–17.

[21] Maskery, I., Hussey, A., Panesar, A., Aremu, A., Tuck, C., Ashcroft, I., and Hague, R., 2017. "An investigation into reinforced and functionally graded lattice structures". *Journal of Cellular Plastics,* **53**(2), pp. 151–165.

[22] Aremu, A., Brennan-Craddock, J., Panesar, A., Ashcroft, I., Hague, R. J., Wildman, R. D., and Tuck, C., 2017. "A voxel-based method of constructing and skinning conformal and functionally graded lattice structures suitable for additive manufacturing". *Additive Manufacturing,* **13**, pp. 1–13.

[23] Brackett, D., Ashcroft, I., and Hague, R., 2011. "A dithering based method to generate variable volume lattice cells for additive manufacturing". In 22nd Annual International Solid Freeform Fabrication Symposium, Austin, TX, Aug, pp. 8–10.

[24] Teufelhart, S., and Reinhart, G., 2012. "Optimization of strut diameters in lattice structures". In 23th Annual Solid Freeform Fabrication Symposium, Austin, TX, pp. 719–733.

[25] Dong, G., Tang, Y., and Zhao, Y. F., 2017. "A survey of modeling of lattice structures fabricated by additive manufacturing". *Journal of Mechanical Design,* **139**(10), p. 100906.

[26] Maskery, I., Aboulkhair, N. T., Aremu, A., Tuck, C., and Ashcroft, I., 2017. "Compressive failure modes and energy absorption in additively manufactured double gyroid lattices". *Additive Manufacturing,* **16**, pp. 24–29.

[27] Meeks, W. H., and Rosenberg, H., 1993. "The geometry of periodic minimal surfaces". *Commentarii Mathematici Helvetici,* **68**(1), pp. 538–578.

[28] Yan, C., Hao, L., Hussein, A., and Young, P., 2015. "Ti–6al–4v triply periodic minimal surface structures for bone implants fabricated via selective laser melting". *Journal of the mechanical behavior of biomedical materials,* **51**, pp. 61–73.

[29] Choy, S. Y., Sun, C.-N., Leong, K. F., and Wei, J., 2017. "Compressive properties of ti-6al-4v lattice structures fabricated by selective laser melting: Design, orientation and density". *Additive Manufacturing,* **16**, pp. 213–224.

[30] Graf, G. C., Chu, J., Engelbrecht, S., and Rosen, D. W., 2009. "Synthesis methods for lightweight lattice structures".

In ASME International Design Engineering Technical Conferences and Computers and Information in Engineering Conference, San Diego, CA, Aug, pp. 579–589.

[31] Pellegrino, S., and Calladine, C. R., 1986. "Matrix analysis of statically and kinematically indeterminate frameworks". *International Journal of Solids and Structures,* **22**(4), pp. 409–428.

[32] Alkhader, M., and Vural, M., 2007. "Effect of microstructure in cellular solids: Bending vs. stretch dominated topologies". In Recent Advances in Space Technologies, 2007. RAST'07. 3rd International Conference on, IEEE, pp. 136–143.

[33] Han, F., Zhu, Z., and Gao, J., 1998. "Compressive deformation and energy absorbing characteristic of foamed aluminum". *Metallurgical and Materials Transactions A,* **29**(10), Oct, pp. 2497–2502.

[34] Smith, M., Guan, Z., and Cantwell, W., 2013. "Finite element modelling of the compressive response of lattice structures manufactured using the selective laser melting technique". *International Journal of Mechanical Sciences,* **67**, pp. 28–41.

[35] Syam, W. P., Jianwei, W., Zhao, B., Maskery, I., Elmadih, W., and Leach, R., 2017. "Design and analysis of strut-based lattice structures for vibration isolation". *Precision Engineering,* **In Press**.

[36] Tanlak, N., De Lange, D. F., and Van Paepegem, W., 2017. "Numerical prediction of the printable density range of lattice structures for additive manufacturing". *Materials & Design,* **133**, pp. 549–558.

[37] Aremu, A., Maskery, I., Tuck, C., Ashcroft, I., Wildman, R., and Hague, R., 2016. "Effects of net and solid skins on self-supporting lattice structures". In *Challenges in Mechanics of Time Dependent Materials, Volume 2*. Springer, pp. 83–89.

[38] Hussein, A., Hao, L., Yan, C., Everson, R., and Young, P., 2013. "Advanced lattice support structures for metal additive manufacturing". *Journal of Materials Processing Technology,* **213**(7), pp. 1019 – 1026.

[39] Qiu, C., Yue, S., Adkins, N. J., Ward, M., Hassanin, H., Lee, P. D., Withers, P. J., and Attallah, M. M., 2015. "Influence of processing conditions on strut structure and compressive properties of cellular lattice structures fabricated by selective laser melting". *Materials Science and Engineering: A,* **628**, pp. 188–197.

[40] Gibson, I., Rosen, D., and Stucker, B., 20115, Second Editio. "Additive manufacturing technologies, 3d printing, rapid prototyping, and direct digital manufacturing, springer". *New York Heidelberg Dordrecht London*.

[41] Yang, L., Harrysson, O., West, H., and Cormier, D., 2015. "Mechanical properties of 3d re-entrant honeycomb auxetic structures realized via additive manufacturing". *International Journal of Solids and Structures,* **69**, pp. 475–490.

[42] Everhart, W., Sawyer, E., Neidt, T., Dinardo, J., and Brown, B., 2016. "The effect of surface finish on tensile behavior of additively manufactured tensile bars". *Journal of materials science,* **51**(8), pp. 3836–3845.

[43] Pyka, G., Kerckhofs, G., Papantoniou, I., Speirs, M., Schrooten, J., and Wevers, M., 2013. "Surface roughness and morphology customization of additive manufactured open porous ti6al4v structures". *Materials,* **6**(10), pp. 4737–4757.

[44] de Formanoir, C., Suard, M., Dendievel, R., Martin, G., and Godet, S., 2016. "Improving the mechanical efficiency of electron beam melted titanium lattice structures by chemical etching". *Additive Manufacturing,* **11**, pp. 71–76.

[45] Ziemian, C., Sharma, M., and Ziemian, S., 2012. "Anisotropic mechanical properties of abs parts fabricated by fused deposition modelling". InTechOpen.

[46] Hutchinson, R., and Fleck, N., 2006. "The structural performance of the periodic truss". *Journal of the Mechanics and Physics of Solids,* **54**(4), pp. 756–782.

[47] Vongbunyong, S., and Kara, S., 2017. "Rapid generation of uniform cellular structure by using prefabricated unit cells". *International Journal of Computer Integrated Manufacturing,* **30**(8), pp. 792–804.

[48] Engelbrecht, S., Folgar, L., Rosen, D. W., Schulberger, G., Williams, J., et al., 2009. "Cellular structures for optimal performance". In Proc. SFF Symposium. Austin, pp. 831–842.

[49] Tang, Y., and Zhao, Y., 2015. "Lattice-skin structures design with orientation optimization". In Proc. Solid Free. Fabr. Symp, pp. 1378–1393.

[50] Reinhart, G., and Teufelhart, S., 2013. "Optimization of mechanical loaded lattice structures by orientating their struts along the flux of force". *Procedia CIRP,* **12**, pp. 175–180. Eighth CIRP Conference on Intelligent Computation in Manufacturing Engineering.

[51] Wu, J., Wang, C. C., Zhang, X., and Westermann, R., 2016. "Self-supporting rhombic infill structures for additive manufacturing". *Computer-Aided Design,* **80**, pp. 32–42.

[52] Kolken, H. M., Janbaz, S., Leeflang, S. M., Lietaert, K., Weinans, H. H., and Zadpoor, A. A., 2018. "Rationally designed meta-implants: a combination of auxetic and conventional meta-biomaterials". *Materials Horizons,* **5**(1), pp. 28–35.

[53] Tang, Y., Tang, Y., Zhao, Y. F., and Zhao, Y. F., 2016. "A survey of the design methods for additive manufacturing to improve functional performance". *Rapid Prototyping Journal,* **22**(3), pp. 569–590.

[54] Choy, S. Y., Sun, C.-N., Leong, K. F., and Wei, J., 2017. "Compressive properties of functionally graded lattice structures manufactured by selective laser melting". *Materials & Design,* **131**, pp. 112 – 120.

[55] Reinhart, G., and Teufelhart, S., 2011. "Load-adapted design of generative manufactured lattice structures". *Physics Procedia,* **12**, pp. 385–392.

[56] Brackett, D., Ashcroft, I., Wildman, R., and Hague, R. J., 2014. "An error diffusion based method to generate functionally graded cellular structures". *Computers & Structures,* **138**, pp. 102–111.

[57] Luxner, M. H., Stampfl, J., and Pettermann, H. E., 2005. "Finite element modeling concepts and linear analyses of 3d regular open cell structures". *Journal of Materials science,* **40**(22), pp. 5859–5866.

[58] Salonitis, K., Chantzis, D., and Kappatos, V., 2017. "A hybrid finite element analysis and evolutionary computation method for the design of lightweight lattice components with optimized strut diameter". *The International Journal of Advanced Manufacturing Technology,* **90**(9-12), pp. 2689–2701.

[59] Labeas, G., and Sunaric, M., 2010. "Investigation on the static response and failure process of metallic open lattice cellular structures". *Strain,* **46**(2), pp. 195–204.

[60] Bici, M., Campana, F., and De Michelis, M., 2017. "Mesoscale geometric modeling of cellular materials for finite element analysis". *Computer-Aided Design and Applications,* **14**(6), pp. 760–769.

[61] Boniotti, L., Beretta, S., Foletti, S., and Patriarca, L., 2017. "Strain concentrations in bcc micro lattices obtained by am". *Procedia Structural Integrity,* **7**, pp. 166–173. 3rd International Symposium on Fatigue Design and Material Defects, FDMD 2017.

[62] Ushijima, K., Cantwell, W., Mines, R., Tsopanos, S., and Smith, M., 2011. "An investigation into the compressive properties of stainless steel micro-lattice structures". *Journal of Sandwich Structures & Materials,* **13**(3), pp. 303–329.

[63] Wong, K. V., and Hernandez, A., 2012. "A review of additive manufacturing". *ISRN Mechanical Engineering,* **2012**.

[64] Frazier, W. E., 2014. "Metal additive manufacturing: a review". *Journal of Materials Engineering and Performance,* **23**(6), pp. 1917–1928.

[65] Yan, C., Hao, L., Hussein, A., and Raymont, D., 2012. "Evaluations of cellular lattice structures manufactured using selective laser melting". *International Journal of Machine Tools and Manufacture,* **62**, pp. 32–38.

[66] Brackett, D., Ashcroft, I., and Hague, R., 2011. "Topology optimization for additive manufacturing". In Proceedings of the solid freeform fabrication symposium, Austin, TX, Vol. 1, S, pp. 348–362.

[67] Wang, Y., Zhang, L., Daynes, S., Zhang, H., Feih, S., and Wang, M. Y., 2018. "Design of graded lattice structure with optimized mesostructures for additive manufacturing". *Materials & Design,* **142**, pp. 114 – 123.

[68] Wang, Y., Chen, F., and Wang, M. Y., 2017. "Concurrent design with connectable graded microstructures". *Computer Methods in Applied Mechanics and Engineering,* **317**, pp. 84–101.

[69] Alexandersen, J., and Lazarov, B. S., 2015. "Topology optimisation of manufacturable microstructural details without length scale separation using a spectral coarse basis preconditioner". *Computer Methods in Applied Mechanics and Engineering,* **290**, pp. 156–182.

[70] Wu, J., Aage, N., Westermann, R., and Sigmund, O., 2018. "Infill optimization for additive manufacturing—approaching bone-like porous structures". *IEEE transactions on visualization and computer graphics,* **24**(2), pp. 1127–1140.

[71] Beyer, C., 2014. "Strategic implications of current trends in additive manufacturing". *Journal of Manufacturing Science and Engineering,* **136**(6), pp. 064701–8.

[72] Panesar, A., Abdi, M., Hickman, D., and Ashcroft, I., 2018. "Strategies for functionally graded lattice structures derived using topology optimisation for additive manufacturing". *Additive Manufacturing,* **19**, pp. 81 – 94.

[73] Hao, L., Raymond, D., Yan, C., Hussein, A., and Young, P., 2011. "Design and additive manufacturing of cellular lattice structures". In The International Conference on Advanced Research in Virtual and Rapid Prototyping (VRAP). Taylor & Francis Group, Leiria, pp. 249–254.

[74] Kantareddy, S., Roh, B., Simpson, T., Joshi, S., Dickman, C., and Lehtihet, E., 2016. "Saving weight with metallic lattice structures: Design challenges with a real-world example". In Solid Freeform Fabrication Symposium (SFF), Austin, TX, Aug, pp. 8–10.

[75] Hadi, A., Vignat, F., and Villeneuve, F., 2015. "Design configurations and creation of lattice structures for metallic additive manufacturing". In 14ème Colloque National AIP PRIMECA.

[76] Segerman, H., 2012. "3d printing for mathematical visualisation". *The Mathematical Intelligencer,* **34**(4), Dec,

pp. 56–62.

[77] Savio, G., Rosso, S., Meneghello, R., and Concheri, G., 2018. "Geometric modeling of cellular materials for additive manufacturing in biomedical field: A review". *Applied Bionics and Biomechanics,* **2018**(1654782), pp. 1–14.

[78] Savio, G., Meneghello, R., and Concheri, G., 2018. "Geometric modeling of lattice structures for additive manufacturing". *Rapid Prototyping Journal,* **24**(2), Mar, pp. 351–360.

[79] ASTM52910-17, I. . Standard guidelines for design for additive manufacturing. Tech. rep., ASTM International, West Conshohocken, PA, 2016, www.astm.org.

[80] Parthasarathy, J., Starly, B., and Raman, S., 2011. "A design for the additive manufacture of functionally graded porous structures with tailored mechanical properties for biomedical applications". *Journal of Manufacturing Processes,* **13**(2), pp. 160–170.

[81] Aversa, R., Petrescu, F. I. T., Petrescu, R. V. V., and Apicella, A., 2016. "Biomimetic finite element analysis bone modeling for customized hybrid biological prostheses development". *American Journal of Applied Sciences,,* **13**(11), pp. 1060–1067.

[82] Murr, L., Gaytan, S., Medina, F., Lopez, H., Martinez, E., Machado, B., Hernandez, D., Martinez, L., Lopez, M., Wicker, R., et al., 2010. "Next-generation biomedical implants using additive manufacturing of complex, cellular and functional mesh arrays". *Philosophical Transactions of the Royal Society of London A: Mathematical, Physical and Engineering Sciences,* **368**(1917), pp. 1999–2032.

[83] Petrovic, V., Vicente Haro Gonzalez, J., Jorda Ferrando, O., Delgado Gordillo, J., Ramon Blasco Puchades, J., and Portoles Grinan, L., 2011. "Additive layered manufacturing: sectors of industrial application shown through case studies". *International Journal of Production Research,* **49**(4), pp. 1061–1079.

[84] Limmahakhun, S., Oloyede, A., Sitthiseripratip, K., Xiao, Y., and Yan, C., 2017. "3d-printed cellular structures for bone biomimetic implants". *Additive Manufacturing,* **15**, pp. 93–101.

[85] de Wild, M., Zimmermann, S., Rüegg, J., Schumacher, R., Fleischmann, T., Ghayor, C., and Weber, F. E., 2016. "Influence of microarchitecture on osteoconduction and mechanics of porous titanium scaffolds generated by selective laser melting". *3D Printing and Additive Manufacturing,* **3**(3), pp. 142–151.

[86] Gao, W., Zhang, Y., Ramanujan, D., Ramani, K., Chen, Y., Williams, C. B., Wang, C. C., Shin, Y. C., Zhang, S., and Zavattieri, P. D., 2015. "The status, challenges, and future of additive manufacturing in engineering". *Computer-Aided Design,* **69**, pp. 65–89.

[87] Wadley, H. N., 2006. "Multifunctional periodic cellular metals". *Philosophical Transactions of the Royal Society of London A: Mathematical, Physical and Engineering Sciences,* **364**(1838), pp. 31–68.

[88] Brooks, H., and Brigden, K., 2016. "Design of conformal cooling layers with self-supporting lattices for additively manufactured tooling". *Additive Manufacturing,* **11**, pp. 16–22.

[89] Ozdemir, Z., Hernandez-Nava, E., Tyas, A., Warren, J. A., Fay, S. D., Goodall, R., Todd, I., and Askes, H., 2016. "Energy absorption in lattice structures in dynamics: Experiments". *International Journal of Impact Engineering,* **89**, pp. 49–61.

[90] Hasib, H., Rennie, A., Burns, N., and Geekie, L., 2015. "Non-stochastic lattice structures for novel filter applications fabricated via additive manufacturing". *Filtration,* **15**(3), pp. 174–180.

[91] Sugimura, Y., 2004. "Mechanical response of single-layer tetrahedral trusses under shear loading". *Mechanics of Materials,* **36**(8), pp. 715–721.

[92] Moongkhamklang, P., Deshpande, V., and Wadley, H., 2010. "The compressive and shear response of titanium matrix composite lattice structures". *Acta Materialia,* **58**(8), pp. 2822–2835.

[93] Ptochos, E., and Labeas, G., 2012. "Shear modulus determination of cuboid metallic open-lattice cellular structures by analytical, numerical and homogenisation methods". *Strain,* **48**(5), pp. 415–429.

[94] Kooistra, G. W., Queheillalt, D. T., and Wadley, H. N., 2008. "Shear behavior of aluminum lattice truss sandwich panel structures". *Materials Science and Engineering: A,* **472**(1-2), pp. 242–250.

[95] Queheillalt, D. T., and Wadley, H. N., 2009. "Titanium alloy lattice truss structures". *Materials & Design,* **30**(6), pp. 1966–1975.

[96] Dong, L., and Wadley, H., 2016. "Shear response of carbon fiber composite octet-truss lattice structures". *Composites Part A: Applied Science and Manufacturing,* **81**, pp. 182–192.

[97] Ion, A., Frohnhofen, J., Wall, L., Kovacs, R., Alistar, M., Lindsay, J., Lopes, P., Chen, H.-T., and Baudisch, P., 2016. "Metamaterial mechanisms". In Proceedings of the 29th Annual Symposium on User Interface Software and Technology, ACM, pp. 529–539.

[98] Bertoldi, K., Vitelli, V., Christensen, J., and van Hecke, M., 2017. "Flexible mechanical metamaterials". *Nature Reviews Materials,* **2**, p. 17066.

[99] Yuan, S., Shen, F., Bai, J., Chua, C. K., Wei, J., and Zhou, K., 2017. "3d soft auxetic lattice structures fabricated by selective laser sintering: Tpu powder evaluation and process optimization". *Materials & Design,* **120**, pp. 317–327.

[100] Li, T., Hu, X., Chen, Y., and Wang, L., 2017. "Harnessing out-of-plane deformation to design 3d architected lattice metamaterials with tunable poisson's ratio". *Scientific Reports,* **7**, p. 8949.

[101] Choi, J., Kwon, O.-C., Jo, W., Lee, H. J., and Moon, M.-W., 2015. "4d printing technology: A review". *3D Printing and Additive Manufacturing,* **2**(4), pp. 159–167.

[102] Bogue, R., 2012. "Smart materials: a review of recent developments". *Assembly Automation,* **32**(1), pp. 3–7.

[103] Gao, B., Yang, Q., Zhao, X., Jin, G., Ma, Y., and Xu, F., 2016. "4d bioprinting for biomedical applications". *Trends in biotechnology,* **34**(9), pp. 746–756.

[104] Gladman, A. S., Matsumoto, E. A., Nuzzo, R. G., Mahadevan, L., and Lewis, J. A., 2016. "Biomimetic 4d printing". *Nature materials,* **15**(4), pp. 413–418.

[105] Meisel, N. A., Elliott, A. M., and Williams, C. B., 2015. "A procedure for creating actuated joints via embedding shape memory alloys in polyjet 3d printing". *Journal of Intelligent Material Systems and Structures,* **26**(12), pp. 1498–1512.

[106] Wagner, M., Chen, T., and Shea, K., 2017. "Large shape transforming 4d auxetic structures". *3D Printing and Additive Manufacturing,* **4**(3), pp. 133–142.

[107] Truby, R. L., and Lewis, J. A., 2016. "Printing soft matter in three dimensions". *Nature,* **540**, pp. 371–378.

[108] Jiang, Y., and Wang, Q., 2016. "Highly-stretchable 3d-architected mechanical metamaterials". *Scientific reports,* **6**, p. 34147.

List of Figures

1 The concept of *lattice* applied to different dimensional scales: structures defining the atoms arrangement in the micro-scale; structures of cellular materials in the meso-scale; specific architectural structures in the macro-scale. 3

2 Cellular structures can be divided into stochastic and non-stochastic ones. Both the arrangement as well as the geometry of the unit cells of 2D and 3D non-stochastic structures can be designed. This paper is focused on the design process of *3D strut-and-node based lattice structures*. This type of cellular structure is highlighted in the image. This figure is inspired by [4], page 325, while the TPMS structure has been modeled using the software, developed at the University of Nottingham, mentioned in [14]. 4

3 The Meso-Scale Lattice Structures (MSLSs) design workflow. Starting from the available design space and the functional targets to be reached, the design process is then structured into five main phases. During these phases manufacturing constraints will also be taken into account to guarantee the printability of the structure. 6

4 Two examples of unit cells: a TPMS (cell modeled using the software, developed at the University of Nottingham, mentioned in [14]) and a 3D strut-and-node based cell. 7

5 The qualitative stress/strain curves of *stretch-dominated* and *bending-dominated* unit cells. The stress/strain curve of *stretch-dominated* unit cells is characterized by high stiffness and high initial strength, followed by post-yield softening. The stress/strain curve of *bending-dominated* unit cells is characterized by a lower stiffness, a lower initial strength and a large deformation at relatively low and constant stress (plateau stress). The last part of both curves shows the densification phase, that is the moment when the struts merge. The image is inspired by the work [1], pages 19 and 26. 8

6 Maxwell's Criterion (see Equation 2). The unit cell on the left has $M<0$: it is *bending-dominated* (nodes are all locked). The unit cell in the centre has $M=0$: it is *stretch-dominated*. Adding a further strut to this cell will make $M>0$. In this case, if nodes are unlocked there is a state of self-stress: the struts carry stress also if no external loads are applied. If nodes are locked, the cell is still *stretch-dominated* and can be manufactured using AM technologies. Figure inspired by [1] page 24. 9

7 Unit cell optimization according to six loading conditions (xx, yy, zz, yz, xy, xz). Considering, as design requirements, the stiffness and the strength as well as the loading conditions, the unit cell is optimized through a proper strut positioning for each loading condition. The combined results lead to the final cell developed and optimized in all directions. Figure inspired by [3] page 153. 10

8 The aspect ratio of a BCC unit cell. When W and, thus, the aspect ratio (W/H) decreases, the unit cell shows higher stiffness and yield stress. In particular, the amplitude of the angles between the struts changes. The amplitude of the angles at the bottom, and at the top of the unit cell, decreases while, for the angles at the sides (α) of the unit cell, the amplitude increases. This figure is used to summarise some considerations provided in [34]. 11

9 The total area moment of inertia values (I) of the cells about centroid coordinate axes. The figure shows how 3 different geometric configurations of unit cells, having the same W, H and D values (respectively 10mm, 10mm, and 1mm), but a different struts number and arrangement, have different I values. 12

10 The figure shows the deviation between the thickness of the virtual model of the struts (black lines) and the additively manufactured ones (dashed red lines) as discussed in [20]: both for horizontal and sloped struts such deviation is related to the change of the D value. For horizontal struts, this value can vary between t_{max} and t_{min}. For sloped struts the cross section is no more a circle but it can vary between t_a and t_b. This figure has been inspired by the work [20], pages 8 and 9. 14

11 The uniform population is based on a periodic unit cell distribution. The figure shows how all unit cells have the same shape and dimensions. Dashed red lines are used to highlight that the unit cells integrity, at the boundary, is accidental. 16

12 The conformal population is based on a distribution of the unit cells that is conformal to the boundaries of the design space. The figure shows that the unit cells do not have the same shape and dimensions. The dashed red lines and the red box highlight that they are fully conformal to the boundaries and their integrity is preserved. 17

13 The figure shows the application of a heterogeneous gradient through the use of a grey scale image that is overlaid to a uniform lattice structure. The darker areas have a higher relative density (through the struts thickening), while the clearer ones have a lower relative density. Both the uniform and graded structures were modeled using the software, developed at the University of Nottingham, mentioned in [14]. 19

14 The figure shows the model that has been used in [34] for performing a FEA on BCC and BCC-Z unit cells. The solid model is based on the use of struts wholly straight and with a constant diameter. A compression test is simulated applying the same loading conditions on the planar face at the top of each unit cell and using a rigid plate to crush the same unit cells progressively. 21

15 The figure shows how shear bands (dashed red lines) can occur when an array of unit cells less regular, like BCC-Z with the characteristic vertical strut in the middle, is loaded (see also Figure 14). In these cases, a simulation performed on a single unit cell can be not sufficient to get information on the deformability of a lattice structure. This image has been inspired by the work [34], page 39. 21